بسم الله الرحمن الرحيم

Sudan University of Science and Technology

College of Graduates Studies

Detection of Liver Diseases in Computed Tomography Scan Images Using Artificial Neural Networks

الكشف عن امراض الكبد في صور المسح الأشعة المقطعية باستخدام الشبكات العصبية الصناعية

A Thesis Submitted in partial fulfillment of the requirement for the M.Sc. Degree in Biomedical Engineering

By:

Sahar Rahamtallah Gadeen

Supervisor:

Dr. Zeinab Adam Mustafa

September - 2016

Sudan University of Science & Technology

College of Graduate Studies

بسم الله الرحمن الرحيم

كلية الدراسات العليا

جامعة السودان للعلوم والتكنولوجيا

كلية الدراسات العليا

Approval Page

Name of Candidate: Sahar Rahmaallah Sadeen Madani

Thesis title: Detection of liver Diseases In Computed Tomography Scan Images Using Artifical Neural Networks

Approved by:

1. External Examiner

Name: Dr. Eltahir Mohamed Hussein

Signature: ..... Date: 29/8/2016

2. Internal Examiner

Name: Magdi B. M. Amin

Signature: ..... Date: 29/8/2016

3. Supervisor

Name: Zenab Adam Mustafa

Signature: ..... Date: 29/8/2016

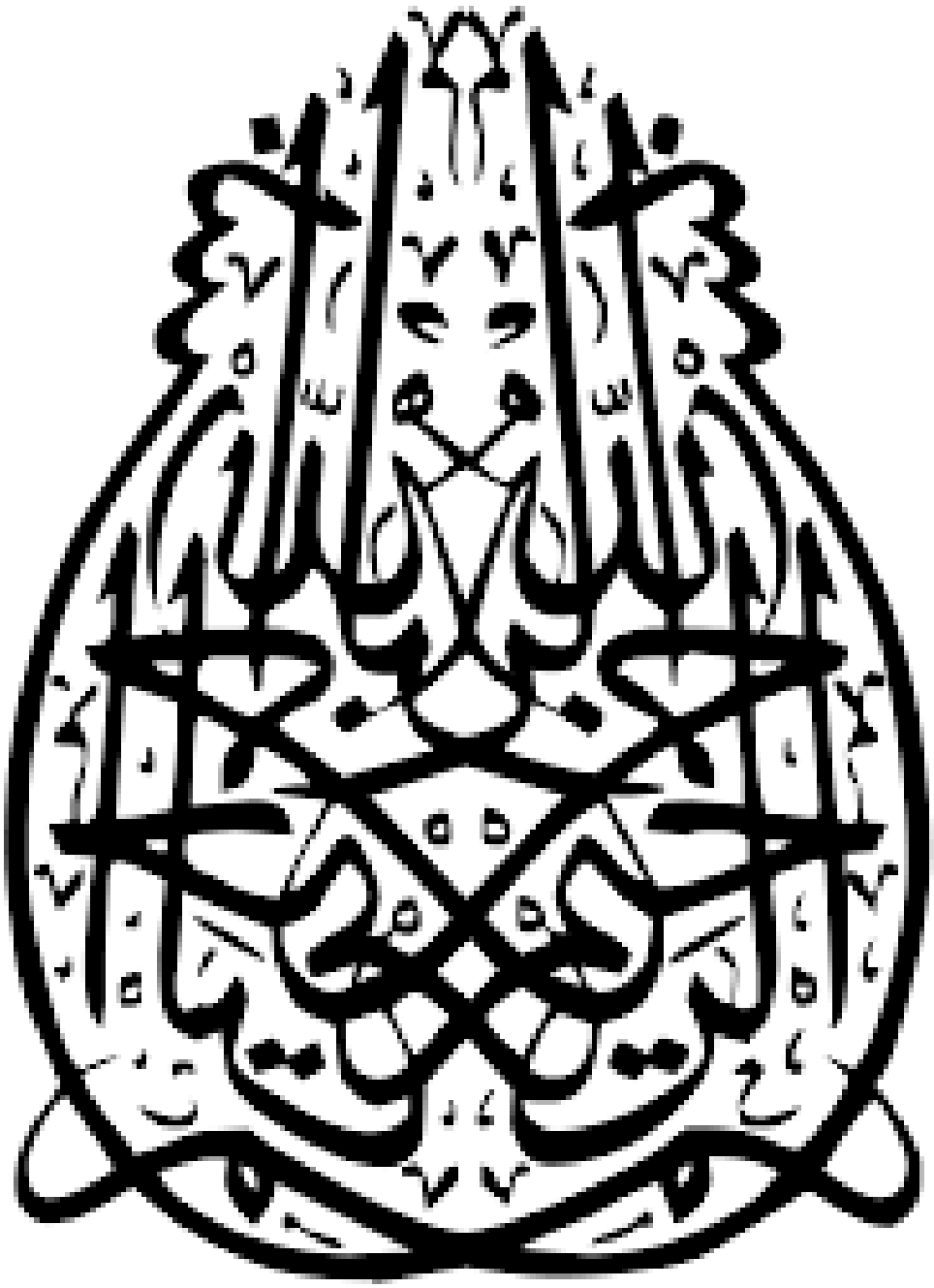

الآية

بسم الله الرحمن الرحيم

(قُل لَّئِنِ اجْتَمَعَتِ الْإِنسُ وَالْجِنُّ عَلَىٰ أَن يَأْتُوا بِمِثْلِ هَٰذَا الْقُرْآنِ لَا يَأْتُونَ بِمِثْلِهِ وَلَوْ كَانَ بَعْضُهُمْ لِبَعْضٍ ظَهِيرًا)

{ سورة الاسراء : الآية 88}

صدق الله العظيم

DEDICATION

I dedicate this thesis to my parents for their endless love, support and encouragement. And especially my mother for her greet effort to make me always on the top.

ACKNOWLEDGMENTS

First and foremost, I have to thank my parents for their love and support throughout my life. Thank you both for giving me strength to reach for the stars and chase my dreams. My lovely sister deserves my wholehearted thanks as well for her continuously support.

I would like to sincerely thank my supervisor Dr. **Zeinb Adm Mustafa,** for her guidance and support throughout this study and especially for her everlasting collaboration and trusting in me.

ABBREVIATIONS

WCRF	World Cancer Research Fund International
CT	Computed Tomography
ANN	Artificial Neural Network
SVM	Support Vector Machine
FNH	Focal Nodular Hyperplasia
HCC	Hepatocellular Cancer
CEUS	Contrast-Enhanced Ultrasound
MDCT	Multi Detector Row Helical Computed Tomography
MRI	Magnetic Resonance Imaging
BSG	British Society of Gastroenterologist
UCAs	Development of Ultrasound Contrast Agents
RES	Reticuloendothelial system
PET	Positron emission tomography
PACS	Archiving and Communication Systems
DICOM	Digital Imaging and Communications in Medicine
MSE	Mean Square Error
PSNR	Peak Signal to Noise Ratio
GLCM	Gray Level Co-occurrence Matrix
SGLDM	Spatial Gray Level Dependence Matrix
GUI	Graphical User Interface

Table of Contents

List of Figures

List of Tables

ABSTRACT

Liver is one of the most important organ in the human body, it performs a variety of vital functions. Liver cancer is a pathological disorder of the human that affects around 50 million people worldwide. The early detection and diagnosis of liver cancer is very important to facilitate the treatment process.

The objective of this study is to design and develop an automated system for liver CT images diagnosis as normal or abnormal to help physicians in their diagnosis and treatment plan.

The proposed system performs an automatic segmentation of liver region after applying different enhancement techniques, then the features are extracted from the segmented liver region using Haralick's feature, this step is followed by features selection and reduction to choose the best representative features. As final step selected features are classified into two classes normal or abnormal.

Artificial Neural Network (ANN) and Support Vector Machine (SVM) are applied in the classification step, then the results of them are compared to each other to select the best one and use it to design an automated system.

المستخلص

الكبد احد اهم الاعضاء في جسم الانسان, فهو يؤدي عدد من الوظائف الحيوية. سرطان الكبد هو خلل مرضي لدى الانسان يصيب حوالي 50 مليون نسمة في العالم. الكشف والتشخيص المبكر لسرطان الكبد مهم جدا لتسهيل عملية العلاج.

الهدف من هذه الدراسة هو تصميم وتطوير نظام ألي لتشخيص صورة الاشعة المقطعية للكبد الى طبيعية أو غير طبيعية لمساعدة الأطباء في تشخيصهم وخطتهم العلاجية.

النظام المقترح يقوم بقطع ألي لمنطقة الكبد من الصورة بعد تطبيق عدد من تقنيات التحسين,بعد ذلك يتم استخلاص ملامح من منطقة الكبد المقطوعة باستخدام (Harlick's features) هذه الخطوة يتبعها انتقاء الملامح الاكثر تمثيلا للبيانات. وكخطوة أخيرة يتم تصنيف هذه الملامح المختارة الى طبيعية او غير طبيعية.

طريقة الشبكات العصبية الصناعية و آلية دعم المتجه تم تطبيقهما في عملية التصنيف,لاحقا تتم مقارنة النتائج المأخوذة من الطريقتين واستخدام افضل طريقة لتصميم النظام المقترح.

CHAPTER ONE

1. INTRODUCTION

1.1 Background:

The liver is the largest gland and largest internal organ in the human body. The liver is a dark red, wedge-shaped gland approximately eight and a half inches long. It is shaped like a pyramid and divided into right and left lobes. Approximately 1.5 L of blood flows through the liver each minute. Liver disease is one of the most serious health diseases that cause death worldwide. As World Cancer Research Fund International (WCRF), liver cancer is the sixth most common cancer in the world, with 782,000 new cases diagnosed in 2012 [1]. In order to give effective treatment to patients, doctors will need to know the features of the tumors. Earlier detection and accurate analysis of liver cancer is an important issue in practical radiology. Liver lesions are a wound or injury to body tissues. It is the area of tissue that caused damage because a wounding or disease. Liver lesions refer to those abnormal tissues that are found in the liver. In a CT scan these can be identified by a difference in pixel intensity from that of the liver [2].

Many clinical applications for computer aided diagnosis require medical images to be segmented. For example, planning of liver tumor embolization, ablation and surgical resection require precise segmentation of the liver from CT images. Due to the complex shape and the large size of this organ, the manual segmentation is time consuming. In order to increase the efficiency of the clinical work, automatic segmentation methods are needed. A computerized liver CT segmentation system should take less time and should

segment the liver accurately. It should be consistent and should provide a system to radiologist which is self-explanatory and easy to operate [3].

Manual segmentation of the CT scans are tedious and time-consuming in a real time clinical situation. Automatic segmentation on the other hand, is a very challenging task, due to various factors, such as liver stretch over 150 slices in a CT image, indefinite shape of the lesions and low intensity contrast between lesions and similar to those of nearby tissues. The irregularity in the liver shape and size between the patients and the similarity with other organs of almost same intensity make automatic liver segmentation difficult [2].

In this study, a liver tumor segmentation algorithm based on feature extraction and SVM classification to detect the tumor more accurately and precisely using an automatic detection method were proposed.

1.2 Problem Statement:

Liver cancer is one of the most common internal malignancies also one of the leading death causes. Computed tomography (CT) has been identified as accurate non-invasive imaging modalities in the diagnosis of the liver cancer, so it is important to diagnose its images effectively and correctly which is difficult to do visually due to low contrast between liver and nearby organs intensities. Liver sometimes presents in different dimensions and makes the detection and segmentation even more difficult.

1.3 Aim of the study:

The objectives of study are divided to general and specific objectives.

1.3.1 General Objective:

The main objective of this research is to classify the liver CT images. An effective and correct diagnosis of liver CT images is very important to avoid faulty in diagnosis which can lead to other problems in treating the patient. The advances in digital image processing techniques have attracted researchers towards the development of computerized methods for liver analysis.

1.3.2 Specific objectives:

The specific objectives are to:

1- Design a computerized system for liver CT images classification.
2- Use a fully automated technique for image segmentation.
3- Support the physicians' decisions for the diagnosis of liver CT images to avoid faulty in diagnosis.
4- Reduce the time required for diagnosis.

1.4 Subject and method:

In this study, a new and accurate method for liver classification from computed tomography (CT) scans is presented. Using MATLAB computerized system consists of four stages is designed. In the first stage of the computerized system, the CT liver image is acquired and preprocessing is done using median filter to remove the noise and to enhance the image contrast. In the second stage, liver region is segmented from the liver CT image using thresholding and morphological operations and then feature extractions are performed over the segmented binary image using Haralick's features texture. In the third stage, post processing enhancement is done on the segmented liver region to enhance the contrast of liver region which

performs a sequence of functions. Finally support vector machine (SVM) and Artificial Neural Network (ANN) classifiers are employed for the classification step.

1.5 Thesis layout:

Chapter one discusses a brief background, problem statement, thesis objectives, and an overview of methodology.

Chapter two will discusses a theoretical background about the methods and techniques of classification and segmentation of liver CT images.

Chapter three discusses the related work of previous studies and a literature reviews.

Chapter four discusses and describes the methodology that was applied for classification of liver CT images.

Chapter five introduces the results that was obtained from the applying of the method which was discussed in chapter four and their discussion.

Chapter six provides the conclusions and recommendations of the thesis.

CHAPTER TWO

2. THEORETICAL BACKGROUND

2.1 liver Background:

The liver is one of the most important organs in the human body. It carries out a variety of functions such as filtering the blood, making bile and proteins, processing sugar, breaking down medications, and storing iron, minerals and vitamins. The liver is prone to many diseases such as hepatitis C, cirrhosis, and cancer. As the advance of computer science and technology, computer aided surgical planning systems have played an important role in diagnosing and treatment of liver diseases. These systems can present the structures of various liver vessels, generate resection proposals, offer 3D visualizations, provide surgical simulations with cutting, and lead to shorter planning times.

2.1.1 Liver Anatomy:

The liver is the largest organ in the abdominal cavity and the most complex. It consists of a myriad of individual microscopic functional units call lobules. The liver performs a variety of functions including the removal of endogenous and exogenous materials from the blood, complex metabolic processes including bile production, carbohydrate homeostasis, lipid metabolism, urea formation, and immune functions.

The liver arises from the ventral mesogastrium and only the upper posterior surface is outside of that structure. The ligamentum teres and falciform ligament connect the liver to the anterior body wall. The lesser omentum connects it to the stomach and the coronary and triangular ligaments to the diaphragm. The liver is smooth and featureless on the diaphragmatic surface

and presents with a series of indentations on the visceral surface where it meets the right kidney, adrenal gland, inferior vena cava, hepatoduodenal ligament and stomach [4].

The liver can be considered in terms of blood supply hepatocytes, Kupffer cells and biliary passages. The liver receives its blood supply from the portal vein and hepatic artery, the former providing about 75% of the total 1500 ml/min flow. Small branches from each vessel—the terminal portal venule and the terminal hepatic arteriole—enter each acinus at the portal triad. Pooled blood then flows through sinusoids between plates and hepatocytes in order to exchange nutrients. The hepatic vein carries efferent blood into the inferior vena cava and a supply of lymphatic vessels drains the liver [4].

Parenchymal cells or hepatocytes comprise the bulk of the organ and carry out complex metabolic processes. Hepatocytes are responsible for the liver's central role in metabolism. These cells are responsible for the formation and excretion of bile; regulation of carbohydrate homeostasis; lipid synthesis and secretion of plasma lipoproteins; control of cholesterol metabolism; and formation of urea, serum albumin, clotting factors, enzymes, and numerous proteins. The liver also aids in the metabolism and detoxification of drugs and other foreign substances.

Kupffer cells line the hepatic sinusoids and are part of the reticuloendothelial system, filtering out minute foreign particles, bacteria, and gut-derived toxins. They also play a role in immune processes that involve the liver.

Biliary passages begin as tiny bile canaliculi formed by hepatocytes. These microvilli -lined structures progress into ductules, interlobular bile ducts, and larger hepatic ducts. Outside the porta hepatis, the main hepatic duct joins the cystic duct from the gallbladder to form the common bile duct, which drains into the duodenum.

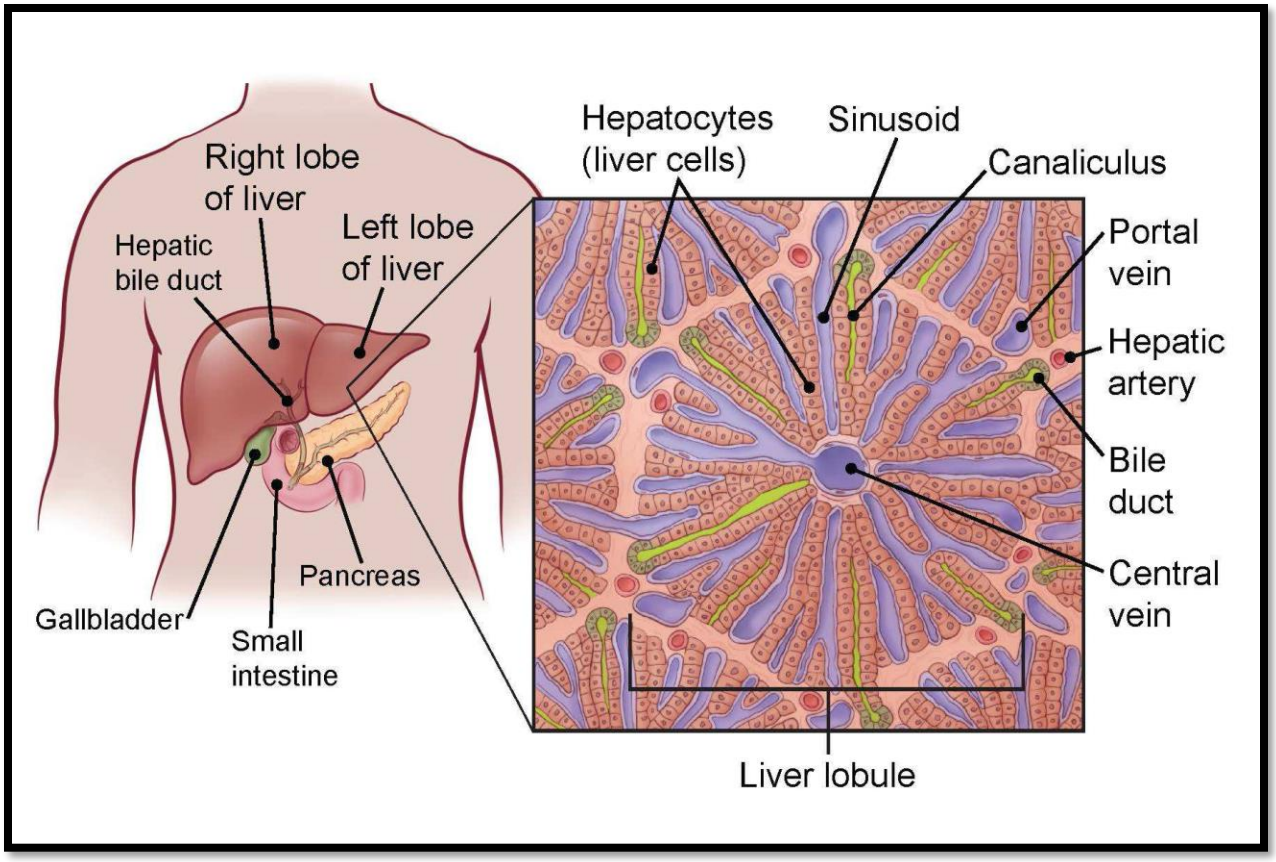

Figure 2.1: Normal gross anatomy of a liver and its histological view [5].

2.1.2 Liver cancer:

These different types of cells in the liver can form several types of malignant (cancerous) and benign (non-cancerous) tumors. These tumors have different causes, are treated differently, and have a different prognosis (outlook) [5].

A. Benign liver tumors:

Benign tumors sometimes grow large enough to cause problems, but they do not grow into nearby tissues or spread to distant parts of the body. If they need to be treated, the patient can usually be cured with surgery. There are different types of benign liver tumors [6]:

1. **Hemangioma:**

The most common type of benign liver tumor, hemangiomas, start in blood vessels. Most hemangiomas of the liver cause no symptoms and do not need treatment. But some may bleed and need to be removed surgically.

2. **Hepatic adenoma:**

Hepatic adenoma is a benign tumor that starts from hepatocytes (the main type of liver cell). Most cause no symptoms and do not need treatment. But some eventually cause symptoms, such as pain or a mass in the abdomen (stomach area) or blood loss. Because there is a risk that the tumor could rupture (leading to severe blood loss) and a small risk that it could eventually develop into liver cancer, most experts will usually advise surgery to remove the tumor if possible.

3. **Focal nodular hyperplasia:**

Focal nodular hyperplasia (FNH) is a tumor-like growth made up of several cell types (hepatocytes, bile duct cells, and connective tissue cells). Although FNH tumors are benign, it can be hard to tell them apart from true liver cancers, and doctors sometimes remove them when the diagnosis is unclear. If you have symptoms from an FNH tumor, it can be removed with surgery. Both hepatic adenomas and FNH tumors are more common in women than in men.

B. Malignant liver tumors:

Malignant liver tumors can be from primary or secondary liver cancer:

Primary liver cancer:

A cancer that starts in the liver is called primary liver cancer. There is more than one kind of primary liver cancer [7]:

1. **Hepatocellular carcinoma (liver cancer):**

This is the most common form of liver cancer in adults Hepatocellular cancer (HCC) can have different growth patterns some begin as a single tumor that grows larger. Only late in the disease does it spread to other parts of the liver. A second type seems to start as many small cancer nodules throughout the liver, not just a single tumor. This is seen most often in people with cirrhosis (chronic liver damage) and is the most common pattern seen in the United States. Using a microscope, doctors can distinguish several subtypes of HCC. Most often these subtypes do not affect treatment or prognosis (outlook). But one of these subtypes, fibrolamellar, is important to recognize. This type is rare, making up less than 1% of HCCs. This type is most often seen in women younger than age 35, and often the rest of the liver is not diseased. This subtype generally has a better outlook than other forms of HCC [8].

Causes Hepatocellular Carcinoma:

The two most important etiological factors contributing to hepatocelluar carcinoma are hepatitis B and hepatitis C. In parts of China and Taiwan, 80% of hepatocellular carcinoma is due to hepatitis B. In the United States and Europe, hepatitis C and hepatitis B contribute equally to disease cases. In Japan, where the prevalence of hepatitis B and hepatitis C is similar, the incidence of hepatocellular carcinoma is higher in patients with hepatitis C compared to hepatitis B (10.4% vs. 3.9%). The pathogenesis of hepatocellular carcinoma in the presence of hepatitis B virus may be due to increased cell turnover from chronic liver disease, or a combination of processes specific to the hepatitis B virus. These may include integration of the hepatitis B DNA genome into the host genome, thereby disrupting the regulatory elements of cell cycling, or via transactivation of host oncogenes by either HBx protein or a truncated protein derived from pre-S2/S region of hepatitis B genome. The

pathogenesis of hepatocellular carcinoma in hepatitis C is less understood. It is possible that some of these patients had previous exposure to hepatitis B virus [9].

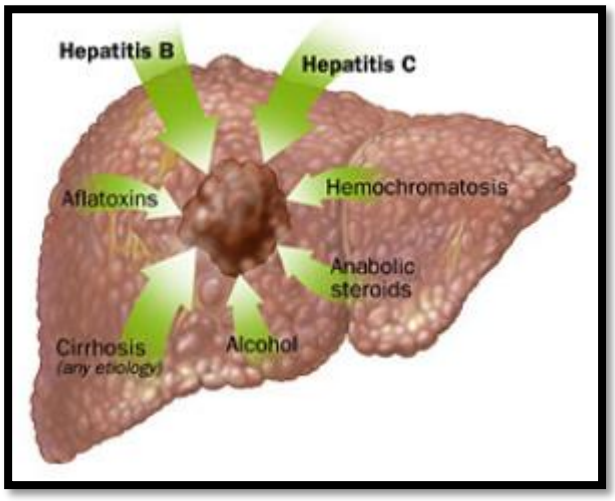

Figure 2.2: Causes of hepatocellular carcinoma [9].

2. Intrahepatic cholangiocarcinoma (bile duct cancer):

About 10% to 20% of cancers that start in the liver are intrahepatic cholangiocarcinomas. These cancers start in the cells that line the small bile ducts (tubes that carry bile to the gallbladder) within the liver. Most cholangiocarcinomas actually start in the bile ducts outside the liver.

Although the rest of this document deals mainly with hepatocellular cancers, cholangiocarcinomas are often treated the same way. For more detailed information on this type of cancer, see our document, Bile Duct (Cholangiocarcinoma) Cancer.

3. Angiosarcoma and hemangiosarcoma:

These are rare cancers that begin in cells lining the blood vessels of the liver. People who have been exposed to vinyl chloride or to thorium dioxide (Thorotrast) are more likely to develop these cancers. See the section "Liver

cancer risk factors" Some other cases are thought to be caused by exposure to arsenic or radium, or to an inherited condition known as hereditary hemochromatosis. In about half of all cases, no likely cause can be identified.

4. Hepatoblastoma:

This is a very rare kind of cancer that develops in children, usually in those younger than 4 years old. The cells of hepatoblastoma are similar to fetal liver cells. About 2 out of 3 children with these tumors are treated successfully with surgery and chemotherapy, although the tumors are harder to treat if they have spread outside the liver.

Secondary liver cancer (metastatic liver cancer):

Most of the time when cancer is found in the liver it did not start there but has spread (metastasized) from somewhere else in the body, such as the pancreas, colon, stomach, breast, or lung. Because this cancer has spread from its original (primary) site, it is a secondary liver cancer. These tumors are named and treated based on their primary site (where they started). For example, cancer that started in the lung and spread to the liver is called lung cancer with spread to the liver, not liver cancer, and it is treated as lung cancer [8].

C. Causes of liver cancer:

Although several risk factors for hepatocellular cancer are known exactly how these may lead normal liver cells to become cancerous is only partially understood. Cancers develop when a cell’s DNA is damaged. DNA is the chemical in each of our cells that makes up our genes – the instructions for how our cells function. Some genes have instructions for controlling when cells grow, divide into new cells, and die [9].

2.2 Liver CT images:

Improvements in imaging technology have allowed exploitation of the dual blood supply of the liver by both the hepatic artery (25%-30%) and portal vein (70%-75%), and the fact that many benign lesions demonstrate characteristic contrast enhancement, due to their vascular supply. Imaging of the liver is often achieved in three distinct phases following intravenous contrast enhancement - the arterial phase, portal venous phase and a late phase. Imaging techniques available include contrast enhanced ultrasound, computed tomography and magnetic resonance imaging [10].

Imaging modalities used in the assessment of liver cancer:

Recent advances in imaging techniques, particularly in the development of Contrast-enhanced ultrasound (CEUS), multidetector row helical computed tomography (MDCT) and MRI contrast agents, have improved detection and characterization of focal liver lesions and enabled accurate staging and appropriate treatment planning in both hepatocellular carcinoma and cholangiocarcinoma. CT and MR remain the imaging techniques of choice for evaluating the liver parenchyma and the presence or absence of distant spread, although CEUS may also be useful in the assessment of vascular invasion [10].

1. **Ultrasound:**

B mode ultrasound (US) is often the first line investigation in liver disease and its use is outlined in the British Society of Gastroenterologist (BSG) guidelines for diagnosis of both HCC and cholangiocarcinoma in adults [11, 12].

CEUS: Progress in both technical advances by ultrasound manufacturers and in the development of ultrasound contrast agents (UCAs) has allowed the role of UCAs to change from Doppler rescue agents to diagnostic agents, providing an assessment of contrast enhancement patterns of liver lesions in real-time. UCAs used in diagnostic US are characterized by a microbubble structure, consisting of gas bubbles stabilized by a shell [13].

UCAs act as blood pool agents allowing the definition and visualization of three overlapping vascular phases-the arterial phase, portal venous phase and late phase, which last until there is clearance of the UCA from the hepatic parenchyma. This late phase differs from the equilibrium phase of extracellular computed tomography (CT) and magnetic resonance imaging (MRI) agents and may reflect sinusoid pooling and reticuloendothelial system (RES) or Kupffer cell uptake[14,15].

2. Computed Tomography (CT):

The development of MDCT, with its superior spatial and temporal resolution, has resulted in improved detection and characterization of focal liver lesions [16]. The acquisition of multiple data sets with each rotation of the x-ray tube in MDCT means the entire liver can be imaged in 10 s or less, compared with 25-30 s for single slice helical CT technology. The short time needed to image the liver allows multiple passes through the liver in different vascular phases following bolus contrast injection and thin-section collimation produces volume data sets with isotropic or near-isotropic voxel dimensions, resulting in superior spatial resolution and the capability to display data in multiple planes. With single-slice helical CT, a ‘dual-phase’ technique is commonly employed with image acquisition in the hepatic arterial-dominant phase and in the portal venous-dominant phase. The ‘triple-phase’ technique includes an early arterial phase, imaged 18-25 s following bolus injection of contrast [17].

Using multiplanar reconstructions, a 3D CT hepatic-mesenteric angiogram can be obtained.

Hypervascular liver lesions are best appreciated in the late arterial phase as they show maximal enhancement relative to the background liver parenchyma. In the portal venous-dominant phase there is maximal parenchymal enhancement with opacification of the hepatic veins. This phase is extended to include the entire abdomen and, depending on the clinical indication, the pelvis. A delayed or equilibrium phase performed 3-5 min following contrast administration may be helpful in further characterizing focal liver lesions.

3. Magnetic Resonance Imaging (MRI):

Although MRI is often viewed as the most sensitive and specific technique for evaluating the liver, this is probably debatable, given the recent revolution in multi-detector CT technology [18, 19]. Nevertheless, lesion/liver contrast is higher for MRI than with CT and the flexibility and range of pulse sequences available in MRI provide a significant advantage over CT. Hepatobiliary MRI uses several magnetic resonance pulse sequences, each of which produces images that provide unique information about the liver and the biliary tree. Most examinations include a T1-weighted in-phase/out-of-phase spoiled gradient echo sequence and one or more T2-weighted sequences. Combining these sequences with extracellular intravenous contrast agents, usually with a fat-saturated spoiled gradient echo sequence, also allows patterns of tumors enhancement to be determined. In addition, use of tissue-specific contrast agents such as super paramagnetic iron oxide, allows improved detection and characterization of liver tumors [20, 21].

4. Positron emission tomography (PET):

The advent of molecular imaging with PET has revolutionized the concept of functional imaging in the management of disease, particularly in the field of oncology, which accounts for 90% of PET applications.

Imaging with PET rather than gamma camera SPECT radiopharmaceuticals allows higher spatial resolution and good image quality, with better detection of even small lesions [22]. PET has the The use of other nuclear medicine techniques in the imaging of liver malignancy, e.g. colloid scintigraphy, has been rendered largely obsolete by improvements in other cross-sectional imaging techniques, principally MRI and US [23].

Table 1: Advantages and Disadvantages of each imaging test [24]:

Image Modality	Advantages	Disadvantages
Ultrasound	Ultrasonography (US) is inexpensive and easily available. It is an excellent test to screen the liver for biliary obstruction or gall bladder disease and to assess vascular patency. It is highly sensitive at differentiating a cyst from a solid liver lesion.	The main limitations of US are high operator dependency, inability to detect lesions <1 cm in size, and low specificity. The presence of diffuse liver disease also lowers the sensitivity of US for the detection of focal lesions.
CT	CT offers the best spatial resolution and the ability to study the entire liver in a single breath-hold. It is an ideal screening examination for the entire abdomen and pelvis. Technological advances in CT technology have further improved the performance of CT scanners in terms of speed of acquisition, resolution, and the ability to image the liver during various	Its limitations include the need for a high radiation dose and a low sensitivity for the detection and characterization of lesions smaller than 1cm. Contrast-enhanced CT is contraindicated in patients with a history of anaphylaxis from contrast agents and renal failure. And it is expensive.

	phases of contrast enhancement more precisely than was possible previously.	
MRI	The main advantages of contrast-enhanced MRI include a high spatial resolution, better contrast sensitivity, better lesion detection and characterization than with CT, and lack of ionizing radiation.	The main drawbacks of MRI include it's a long procedure time, and the need for the patient to hold his breath for longer periods. And it is very expensive.
PET	This procedure is highly sensitive; however, any focal area of hyper-metabolism can give false-positive results. The advantages are its high sensitivity and the ability to survey the entire body at a single sitting.	The main disadvantages include its high cost, poor availability, poor lesion localization, and limited sensitivity for lesions smaller than 1cm.

2.3 Image processing:

Image Processing is a technique to enhance raw images received from cameras/sensors placed on satellites, space probes and aircrafts or pictures taken in normal day-to-day life for various applications. Various techniques have been developed in Image Processing during the last four to five decades. Most of the techniques are developed for enhancing images obtained from unmanned space-crafts, space probes and military reconnaissance flights. Image Processing systems are becoming popular due to easy availability of powerful personnel computers, large size memory devices, graphics software's etc. [25].

By the increasing use of direct digital imaging systems for medical diagnostics, digital image processing becomes more and more important in health care. In addition to originally digital methods, such as Computed Tomography (CT) or Magnetic Resonance Imaging (MRI), initially analogue

imaging modalities such as endoscopy or radiography are nowadays equipped with digital sensors. Digital images are composed of individual pixels (this acronym is formed from the words “picture” and “element”), to which discrete brightness or color values are assigned. They can be efficiently processed, objectively evaluated, and made available at many places at the same time by means of appropriate communication networks and protocols, such as Picture Archiving and Communication Systems (PACS) and the Digital Imaging and Communications in Medicine (DICOM) protocol, respectively. Based on digital imaging techniques, the entire spectrum of digital image processing is now applicable in medicine [26].

2.3.1 Preprocessing:

Medical imaging modalities are basically imaging techniques used to create images of the human body parts for clinical purposes to reveal, diagnose or examine disease and for study of normal anatomy and physiology. However, the different medical imaging modalities still present some disadvantages, such as speckle noise [27], [28], [29] , low contrast or diffuse region boundaries, which may reduce their reliability and make it difficult to apply robust methods for further processing of images like segmentation, feature extraction and computer aided diagnosis.

Image pre-processing is the name for operations on images at the lowest level of abstraction whose aim is an improvement of the image data that suppress undesired distortions or enhances some image features important for further processing. It does not increase image information content. Its methods use the considerable redundancy in images. Neighboring pixels corresponding to one object in real images have the same or similar brightness

value and if a distorted pixel can be picked out from the image, it can be restored as an average value of neighboring pixels [30] [31].

Low image quality is an obstacle for effective analysis, recognition, segmentation, feature extraction and quantitative measurements. Therefore, it is necessary to improve contrast and suppress such noises while retaining as much as possible the important image features for more accurate diagnosis. There are numbers of metrics are available to assess the performance of the filters, but Mean square error (MSE) and Peak signal to noise ratio (PSNR) are the commonly used parameters [31], [29].

2.3.2 Image enhancement:

Image enhancement, which transforms digital images to enhance the visual information within, is a primary operation for almost all vision and image processing tasks in several areas such as computer vision [31]. In many situations, images are mostly affected by mixed noise which is a combination of impulsive noise and additive noise [30].

Image enhancement improves the quality (clarity) [31] of images for human viewing. It basically improves the interpretability or perception of information in images for human viewers and providing `better' input for other automated image processing techniques. The principal objective of image enhancement is to modify attributes of an image to make it more suitable for a given task and a specific observer. During this process, one or more attributes of the image are modified. The choice of attributes and the way they are modified are specific to a given task. Removing blurring and noise, increasing contrast, and revealing details are examples of enhancement operations. For example, an image might be taken of an endothelial cell, which might be of low contrast and somewhat blurred. Reducing the noise and blurring and increasing the

contrast range could enhance the image. The original image might, have areas of very high and very low intensity, which mask details. An adaptive enhancement algorithm reveals these details. Adaptive algorithms adjust their operation based on the image information (pixels) being processed. In this case the mean intensity, Contrast and sharpness (amount of blur removal) could be adjusted based on the pixel intensity statistics in various areas of the image. There exist many techniques that can enhance a digital image without spoiling it [31].

2.3.4 Noise reduction and removal:

Image noises may be caused by faults in camera sensor and environment conditions which are often not possible to avoid in practical situations and atmospheric disturbances are the common causes for impulsive noise, whereas the thermal effect of various electronic circuits and random photon-fluctuation of photo-electronic devices will typically introduce additive noise to images. It is obvious that noise contamination will significantly decrease the visual quality and affect the performance of image-processing techniques. Therefore, image de-noising or filtering is necessary or even indispensable for any image application system and is one of the most common image-processing tasks [32] [33].

Image de-noising is a vital image processing task i.e. as a process itself as well as a component in other processes. There are many ways to de-noise an image or a set of data and methods exists. The important property of a good image de-noising model is that it should completely remove noise as far as possible as well as preserve edges. Traditionally, there are two types of models i.e. linear model and non-liner model. Generally, linear models are used. The benefits of linear noise removing models is the speed and the limitations of

the linear models is, the models are not able to preserve edges of the images in an efficient manner i.e. the edges, which are recognized as discontinuities in the image, are smeared out. On the other hand, Non-linear models can handle edges in a much better way than linear models [34].

2.4.5 Image segmentation:

Liver CT image segmentation is to extract the liver department from all CT images, in order to provide a reliable basis for research for clinical treatment and pathology. Liver CT image segmentation mainly uses the threshold. This segmentation is based on the regional property of the image or its transform; and can also consider the neighborhood characteristics of liver CT image, and use the texture analysis approach to segmentation.

Manual liver segmentation task is not only time consuming and tedious due to the high number of slices but also depends on the skills and experience. Therefore, despite the problematic nature of organ segmentation, automated segmentation methods are needed especially for organs like liver [35].

Liver image segmentation has played a very importance role in medical imaging field. The advances in digital image processing techniques have attracted researchers towards the development of computerized methods for liver analysis. It is the first and essential step for diagnosis of liver tumors, liver surgical planning system such as a system for liver transplantation and 3D liver volume rendering.

Manual segmentation of liver is possible but it is huge time consuming and a cost intensive task and also depends on operator variability. Machine learning techniques combined with image processing techniques provide various semi-automatic and automatic techniques for liver image segmentation. However, liver image segmentation from abdominal images is difficult task due to three

main reasons. First is due to low contrast and blurry edges of liver. Second, intensity of pixels in liver region is similar and overlapped with nearby organs and tissues in abdominal image.

Third, liver is non-rigid in shape and variant in position and it is very complex. All these facts increase the difficulty of the liver image segmentation task [35].

2.3.6 Post-processing:

Image post-processing belongs to the domain of digital image processing, which is simply the processing of images using a digital computer. Film-based radiology is now obsolete and has evolved into various digital imaging modalities, including computed radiography, flat-panel digital radiography, digital fluoroscopy, digital mammography, computed tomography (CT), magnetic resonance imaging (MRI), nuclear medicine, and diagnostic medical sonography. Thus, digital image processing in radiology has become one of the routine skills of technologists and radiologists alike. In addition, the use of the CT and MRI scanners has become an integral imaging component in radiation treatment planning. Therefore, it is important that technologists understand the nature and scope not only of digital images but also of digital image processing, to become effective and efficient users of the new technologies that have made a significant impact on the care and management of patients. The major goal of digital image post-processing in medical imaging is to alter or change an image to enhance diagnostic interpretation [30].

2.3 Texture analysis:

Texture is a combination of repeated patterns with regular/irregular frequency. It can only be visualized but hard to describe in words. Liver

structure exhibit similar behavior; it has maximum disparity in intensity texture inside and along boundary which serves as a major problem in its segmentation and classification. Problem gets more complicated when one applies simple segmentation techniques without considering variation in intensity texture. The problem of representing liver texture is solved by encoding it in terms of certain parameters for texture analysis. Numerous textural analysis techniques have been devised for liver classification over the years some of which work equally work well for most of the imaging modalities.

2.5 Texture features:

Feature extraction is the first stage of image texture analysis. Results obtained from this stage are used for texture discrimination, texture classification or object shape determination.

In statistical texture analysis, texture features are computed from the statistical distribution of observed combinations of intensities at specified positions relative to each other in the image. According to the number of intensity points (pixels) in each combination, statistics are classified into first-order, second-order and higher-order statistics [35].

2.5.1 Gray Level Co-occurrence Matrix:

The Gray Level Co-occurrence Matrix (GLCM) method is a way of extracting second order statistical texture features. A GLCM is a matrix where the number of rows and columns is equal to the number of gray levels, G, in the image. The matrix element P (i , j | x, y) is the relative frequency with which two pixels, separated by a pixel distance (x, y), occur within a given neighborhood, one with intensity i and the other with intensity j. One may also say that the matrix element P (i, j | d, θ) contains the second order statistical

probability values for changes between gray levels i and j at a particular displacement distance d and at a particular angle (θ).

Fig. 2.3 illustrates the details of the process to generate four symmetrical co-occurrence matrices considering a 4×4 image represented with four gray-tone values from 0 to 3. For the purpose we considered one neighboring pixel (d=1) along four possible directions as {[0 1] for 0°; [-1 1] for 45°; [-1 0] for 90° and [-1 -1] for 135°]}.

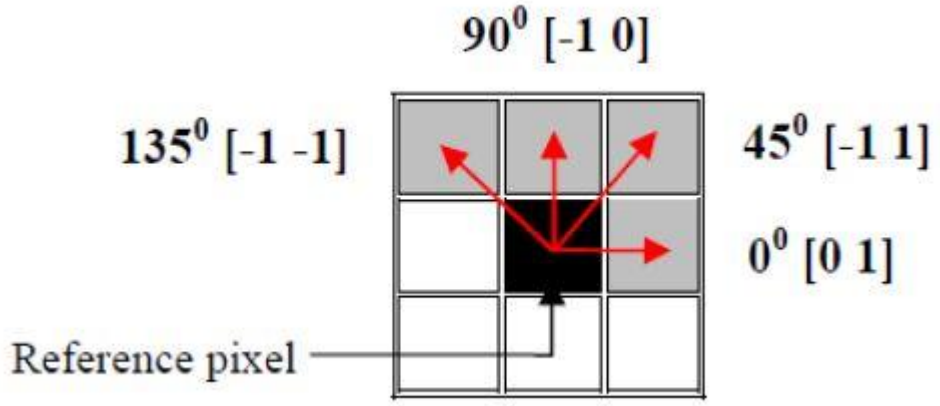

Figure 2.3: Co-occurrence matrix directions for extracting texture features.

Each element of the GLCM is the number of times that two pixels with gray tone i and j are neighborhood in distance d and direction θ. For 0° co-occurrence matrix, there are 2 occurrences of the pixel intensity value 1 and pixel intensity value 3 adjacent to each other in the input image. Also, the occurrence of pixel intensity value 3 and pixel intensity value 1 adjacent to each other is 2 times. Hence, these matrices are symmetric in nature and the co-occurring pairs obtained by choosing θ equal to 0° would be similar to those obtained by choosing θ equal to 180°. This concept extends to 45°, 90° and 135° as well [36].

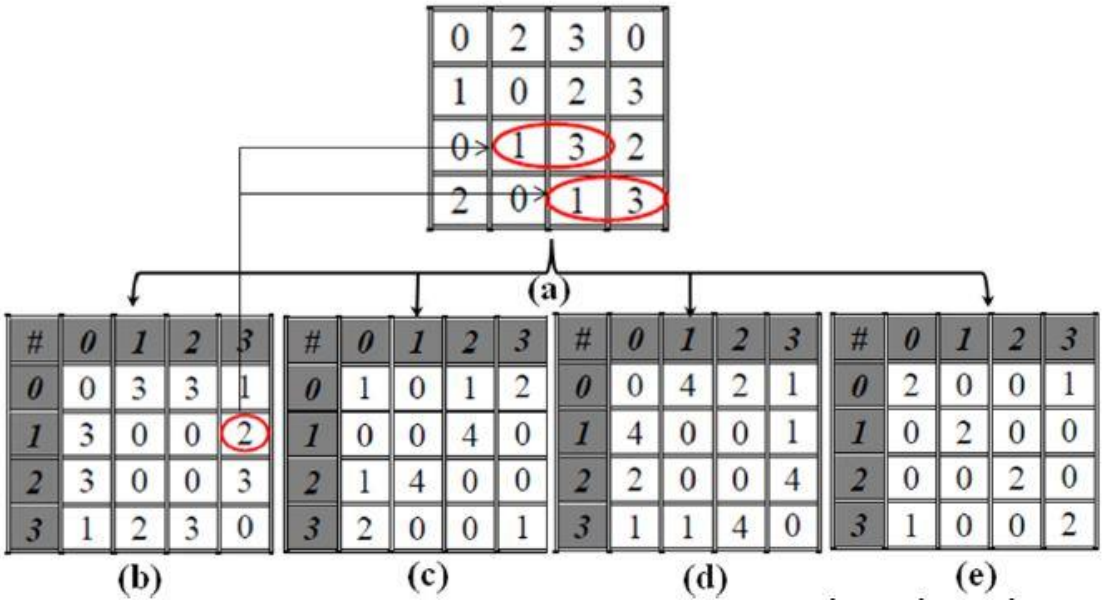

Figure 2.4: GLCM construction based on a (a) test image along four possible directions (b) 0° (c) 45° (d) 90° and (e) 135° with a distance

Haralick et al. introduced 14 statistical features which are generated by calculating the co-occurrence matrix for different directions. These matrices are usually used to characterize textures in an image as it contains information about the image such as homogeneity, contrast, energy, entropy, etc. In the spatial case, its principal diagonal is related to homogeneous regions and the non-zero elements far from it represents high contrast occurrences.

2.5.2 Haralick's Textural Features:

There are three kinds of visual causes people naturally look for in an image: spectral (average tonal variation in various bands of visible wavelengths), contextual (macro data surveyed from surrounding data), and textural. Textural information, or the spatial distribution of tonal variation within a

band, is one of the most important characteristics used in identifying objects or regions of interest in an image.

In our case, texture also represents a natural choice for automated image classification because it avoids the need for both color and context. In 1973, Haralick, Shanmugam, and Dinstein introduced a set of 13 texture features calculated from an image's gray-level co-occurrence matrix (GLCM) [36].

These Haralick features, which are still widely used today for a range of applications, allow quantification of a texture, defined as:

1. Energy:

Energy is a measure of local homogeneity and therefore it represents the opposite of the Entropy. Basically this feature tells how uniform the texture is.

$$\text{Energy} = \sum_{i}^{Ng}\sum_{j}^{Ng}\{p(i,j)\}^2 \dots\dots\dots\dots\dots\dots\dots\dots\dots\dots\dots 1$$

2. Contrast or Inertia:

Contrast is a local grey level variation in the grey level co-occurrence matrix. It can be thought of as a linear dependency of grey levels of neighboring pixels.

$$\text{Contrast} = \sum_{i}^{Ng}\sum_{j}^{Ng}(i,j)^2 p(i,j) \dots\dots\dots\dots\dots\dots\dots\dots\dots\dots\dots 2$$

3. Entropy:

Entropy in any system represents disorder, where in the case of texture analysis is a measure of its spatial disorder.

$$\text{Entropy} = \sum_{i}^{Ng}\sum_{j}^{Ng} p(i,j)\log(p(i,j)) \quad \ldots\ldots\ldots\ldots\ldots\ldots\ldots\ldots\ldots\ldots 3$$

4. Correlation:

The descriptor Correlation (CO) measures the linear dependence of gray level values in the co-occurrence matrix or describes the correlations between the rows and columns of the co-occurrence matrix. This parameter is specified by the following equation:

$$\text{correlation} = \sum_{i}^{N}\sum_{j}^{N} \frac{(i-\mu x)\,(j-\mu y\,)p(i,j)}{\sigma x \sigma y} \quad \ldots\ldots\ldots\ldots\ldots\ldots 4$$

Where μx, μy, σx and σy are the means and standers deviations of px and py.

5. Variance:

Variance is a measure that defines the variation of grey level pairs in an image. It is the closest to Contrast with a difference in the weight – Contrast unlike Dissimilarity grows quadratically.

$$\text{Variance} = \sum_{i,j} |i-j|\, p(i,j) \quad \ldots\ldots\ldots\ldots\ldots\ldots\ldots\ldots\ldots\ldots 5$$

6. Inverse Difference Moment:

Inverse Difference Moment or Homogeneity measures the uniformity of the non-zero entries in the GLCM. It weights values by the inverse of contrast weight.

$$\text{Homogenity} = \sum_{i,j} \frac{1}{1-|i-j|^2}\, p(i,j) \ldots\ldots\ldots\ldots\ldots\ldots\ldots 6$$

7. Sum Average (SA):

$$\mathrm{SA} = \sum_{k=0}^{2N_g-2} k p_{x+y}(k) \quad \ldots\ldots\ldots\ldots\ldots\ldots\ldots\ldots\ldots\ldots\ldots\ldots 7$$

8. Sum Variance (SV):

$$SV = \sum_{k=0}^{2N_g-2} (k - SA)^2 \, p_{x+y}(k) \quad \ldots\ldots\ldots\ldots\ldots\ldots\ldots\ldots\ldots\ldots\ldots\ldots 8$$

9. Sum Entropy (SE):

$$\mathrm{SE} = \sum_{k=0}^{2N_g-2} p_{x+y}(k) \log p_{x+y}(k) \quad \ldots\ldots\ldots\ldots\ldots\ldots\ldots\ldots\ldots\ldots\ldots\ldots 9$$

10. Difference Variance (DV):

$$SV = \sum_{k=0}^{2N_g-1} (k - DA)^2 \, p_{x-y}(k) \quad \ldots\ldots\ldots\ldots\ldots\ldots\ldots\ldots\ldots\ldots\ldots\ldots 10$$

11. Difference Entropy (DE):

$$\mathrm{SE} = \sum_{k=0}^{2N_g-1} p_{x-y}(k) \log p_{x-y}(k) \ldots\ldots\ldots\ldots\ldots\ldots\ldots\ldots\ldots\ldots\ldots\ldots 11$$

12. Difference Average (DA):

$$\mathrm{SA} = \sum_{k=0}^{2N_g-1} kp_{x-y}(k) \ldots\ldots\ldots\ldots\ldots\ldots\ldots\ldots\ldots\ldots\ldots\ldots\ldots\ldots 12$$

13. Information Measures of Correlation (inf1):

$$\inf 1 = \frac{\mathrm{HXY} - \mathrm{HXY1}}{\max\{\mathrm{HX}, \mathrm{HY}\}} \ldots\ldots\ldots\ldots\ldots\ldots\ldots\ldots\ldots\ldots\ldots\ldots\ldots 13$$

14. Information Measures of Correlation inf2:

$$\inf 2 = (1 - \mathrm{e}^{[-2.0(\mathrm{HXY2}-\mathrm{HXY})]})^{1/2} \ldots\ldots\ldots\ldots\ldots\ldots\ldots\ldots 14$$

$$\mathrm{HXY} = \sum_{\mathrm{i}}^{\mathrm{Ng}} \sum_{\mathrm{j}}^{\mathrm{Ng}} \mathrm{p(i,j)log(p(i,j))} \ldots\ldots\ldots\ldots\ldots\ldots\ldots\ldots\ldots 15$$

$$\mathrm{HXY\ 1} = \sum_{\mathrm{i}}^{\mathrm{Ng}} \sum_{\mathrm{j}}^{\mathrm{Ng}} \mathrm{p(i,j)log\{p_x\, i\ p_y\, j\}} \ldots\ldots\ldots\ldots\ldots\ldots\ldots\ldots 16$$

$$\mathrm{HXY\ 2} = \sum_{\mathrm{i}}^{\mathrm{Ng}} \sum_{\mathrm{j}}^{\mathrm{Ng}} \mathrm{p_x\, i\ p_y(j)\ log\{p_x\, i\ p_y\, j\}} \ldots\ldots\ldots\ldots\ldots\ldots 17$$

2.5 Image classification:

The overall objective of image classification is to automatically categorize all pixels in an image into land cover classes or themes. Normally, multispectral data are used to perform the classification, and the spectral pattern present within the data for each pixel is used as numerical basis for categorization. That is, different feature types manifest different combination of DNs based on their inherent spectral reflectance and emittance properties.

The term *classifier* refers loosely to a computer program that implements a specific procedure for image classification. Over the years' scientists have devised many classification strategies. From these alternatives the analyst must select the classifier that will best accomplish a specific task. At present it is not possible to state that a given classifier is "best" for all situations because characteristics of each image and the circumstances for each study vary so greatly. Therefore, it is essential that the analyst understands the alternative strategies for image classification.

The traditional methods of classification mainly follow two approaches: unsupervised and supervised. The unsupervised approach attempts spectral grouping that may have an unclear meaning from the user's point of view.

Having established these, the analyst then tries to associate an information class with each group. The unsupervised approach is often referred to as clustering and results in statistics that are for spectral, statistical clusters. In the supervised approach to classification, the image analyst supervises the pixel categorization process by specifying to the computer algorithm; numerical descriptors of the various land cover types present in the scene. To do this, representative sample sites of known cover types, called training areas or training sites, are used to compile a numerical interpretation key that describes the spectral attributes for each feature type of interest. Each pixel in the data set is then compared numerically to each category in the interpretation key and labeled with the name of the category it looks most like. In the supervised approach the user defines useful information categories and then examines their spectral separability whereas in the unsupervised approach he first determines spectrally separable classes and then defines their informational utility [37].

2.5.1 Artificial Neural Network (ANN):

An artificial neuron is a computational model inspired in the natural neurons. Natural neurons receive signals through *synapses* located on the dendrites or membrane of the neuron. When the signals received are strong enough (surpass a certain *threshold*), the neuron is *activated* and emits a signal though the *axon*. This signal might be sent to another synapse, and might activate other neurons.

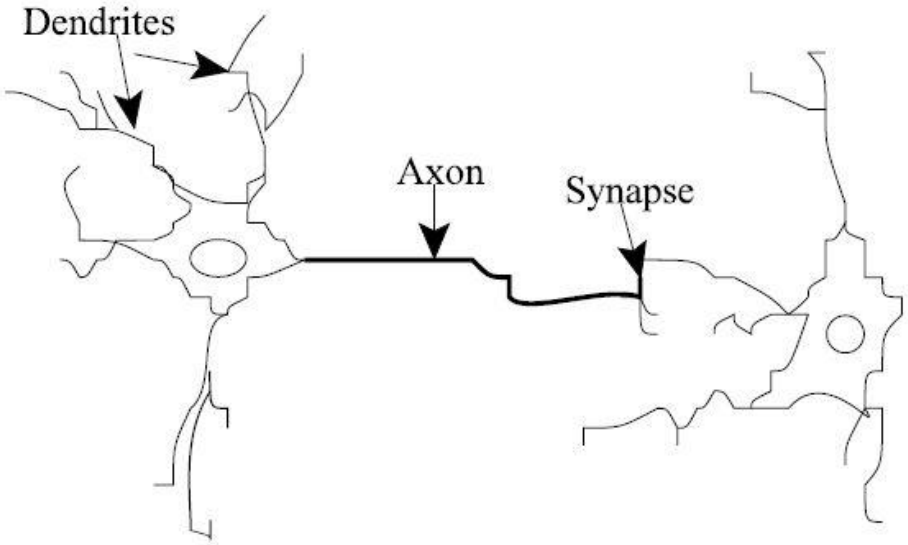

Figure 2.4: Natural Neurons

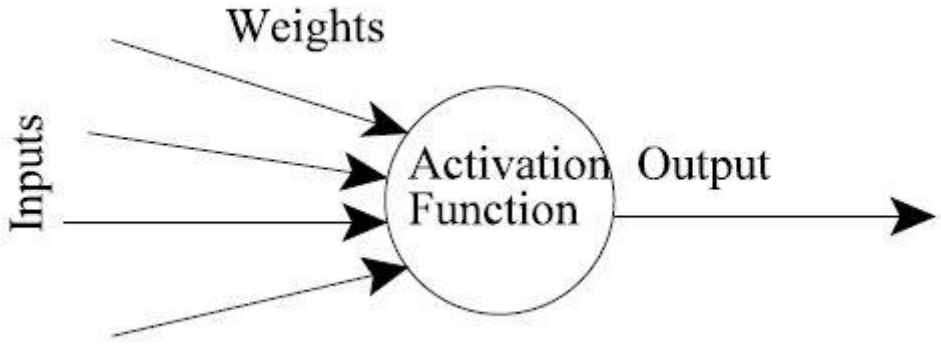

Figure 2.5: An Artificial Neuron

An artificial neural network (ANN) is a computational model that attempts to account for the parallel nature of the human brain. An (ANN) is a network of highly interconnecting processing elements (neurons) operating in parallel. These elements are inspired by biological nervous systems. As in nature, the connections between elements largely determine the network function. A subgroup of processing element is called a layer in the network. The first layer is the input layer and the last layer is the output layer. Between the input and output layer, there may be additional layer(s) of units, called hidden layer(s) [38] show in figure (2.6). The weights in an ANN express the relative strengths (or mathematical values) of the various connections that transfer data from layer to layer. In other words, the weights express the relative importance of each input to a Processing element.

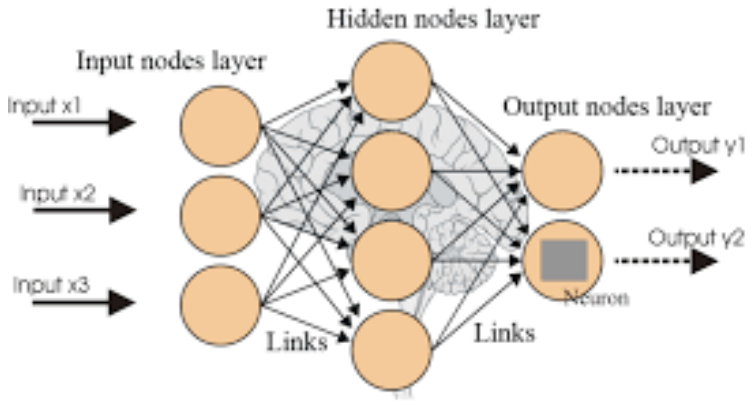

Figure 2.6: Artificial Neural Network

2.5.1 Support Vector Machine (SVM):

The original SVM algorithm was invented by Vladimir Vapnik in 1992, and the current soft margin version was proposed by Vapnik and Cortes in 1995 [39]. A robust method for data classification was implemented via LIBSVM,

an open source machine-learning library developed at the National Taiwan University [40]. LIBSVM implements the sequential minimal optimization (SMO) algorithm for kernelized SVMs, invented by John Platt in 1998 at Microsoft Research [39]. SVMs have enjoyed empirically good performance since then with applications in fields ranging from bioinformatics to text recognition.

SVM is a supervised learning algorithm, meaning it infers its function from labeled training data. In our case, training data is projected into low-dimensional feature space from its original high-dimensional space, and labeled according to one of three possible cases. The goal is to solve for a separating hyper-plane or decision boundary with maximum margins on either side that separates the data classes such that as much of our data as possible is as far away from our decision boundary as possible, thus increasing our prediction probability or confidence. The data points that lie on either margin line, running parallel to the decision boundary, are called the support vectors. These decision boundaries can be linear or nonlinear, and the data can be separable or non-separable.

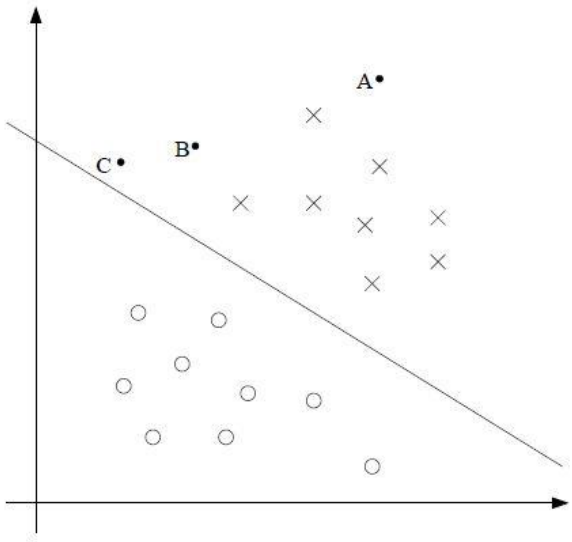

Figure 2.7: separating hyper plane of SVM.

For a different type of intuition, consider the following figure, in which x's represent positive training examples, o's denote negative training examples, a decision boundary (this is the line given by the equation $\theta x = 0$, and is also called the separating hyperplane) is also shown, and three points have also been labeled A, B and C. Notice that the point A is very far from the decision boundary. If we are asked to make a prediction for the value of y at A, it seems we should be quite confident that $y = 1$ there. Conversely, the point C is very close to the decision boundary, and while it's on the side of the decision boundary on which we would predict $y = 1$, it seems likely that just a small change to the decision boundary could easily have caused our prediction to be $y = 0$. Hence, we're much more confident about our prediction at A than at C. The point B lies in-between these two cases, and more broadly, we see that if a point is far from the separating hyperplane, then we may be significantly more confident in our predictions. Again, informally we think it'd be nice if, given a training set, we manage to find a decision boundary that allows us to make all correct and confident (meaning far from the decision boundary) predictions on the training examples.

CHAPTER THREE

3. LITERATURE REVIEW

A considerable percentage of liver texture analysis techniques are based on CT data. Many authors have put their efforts in evaluating and deriving useful information from CT liver images. Mir et al., in their work [41], characterized CT liver images into normal, visible and invisible malignancy. Their approach was based only on an insightful observation of features extracted using SGLDM, RUNL and GLDS. Twenty CT images from each class were used for computing an average value of features by aforementioned techniques. A keen observation revealed that features of ENT, LH and GLD play their discrimination role.

Mala et al. work was a major effort to recognize diffused liver diseases. For this purpose, they developed an automatic liver segmentation and classification system [42] using CT scan data. Bharathi et al. [43] utilized the better feature representation capability and least information redundancy of Zernike moments and Legendre moments for classification of normal and HCC liver using CT images. Total 200 ROI were used out of which 140 belong to healthy liver class and 60 to HCC.

Authors of [44] proposed an automatic liver segmentation method by using pixel based feature extraction, SVM based classification and morphological operations. Wavelet transform [45] was used for feature extraction instead of Fourier [46] and

Gabor [47] because it represents texture at multiple scales. Pixel based features thus obtained serve as input to SVM classifier. SVM based classification does not cater spatial information and second, it heavily

misclassifies pixels. To avoid these problems, well-chosen morphological operations were used in sequence: 1) dilation and erosion with square structuring element six pixels wide, 2) removing areas other than largest, 3) holes filling, 4) removing spurs, and finally 5) erosion and dilation.

Wu et al. proposed a novel approach [48] based on statistical moments for texture analysis. They evaluated Legendre, Zernike, Krawtchouk and chebichef moments [49, 50, and 51] for texture feature extraction in local neighborhood of each pixel. After proving discrimination capability of these moments for standard Brodatz textures, they were applied on CT liver images for tumor recognition. The texture features, calculated using aforementioned moments, for multiphase CT liver images were classified using SVM. Krawtchouk moments were best in terms of classification accuracy.

Abdel-massieh et al. [49] presented a fully automatic method to segment the tumors in liver structure with no interaction from user. Each slice of segmented liver is subjected to contrast enhancement, and then a white image with some pepper noise and tumors as dark gray spots is added. Following Gaussian smoothing, the image is converted into binary with tumors as black spots on white background using Isodata threshold. The experiment was reported on abdominal datasets which showed better results.

An interactive method for liver tumor segmentation from computed tomography (CT) scans is proposed in [50]. After some pre-processing operations, the CT volume is partitioned into a large number of catchment basins under watershed transform. Support vector machines (SVM) classifier is trained to extract tumors from liver image, while the corresponding feature vector for training and prediction is computed based upon each small region produced by watershed transform. Their method was tested and evaluated on MICCAI 2008 liver tumor segmentation challenge datasets.

A semi-automatic segmentation based on non-parametric intensity distribution estimation and a hidden Markov measure field model with a spherical shape has been proposed by Hame and Pollari [51]. A post-processing operation has been presented to remove the overflow to adjacent tissue. The accuracy of the method was validated with two sets of patient data, and artificially generated samples. Their method achieved very high accuracy with the RFA data, and outperformed other methods evaluated with the public data set, thus, receiving an average overlap error of 30.3%. The average volume difference was 23.5%, and the average, the RMS, and the maximum surface distance errors were 1.87, 2.43, and 8.09 mm, respectively. Their experimental results were good even for tumors with very low contrast and ambiguous borders, and the performance remained high with noisy image data.

CHAPTER FOUR

4. METHODOLOGY

4.1 Overview of Methodology:

This chapter provides an obvious illustration of the methods that were applied in this study. The technique of the proposed system of this research can be summarized in five steps. The first step removes the noise from the image, the second step segments the liver portion from the CT image and in the third step post processing using adaptive histogram equalization, Gaussian smoothing and gray level transformations takes place, after that features were extracted from segmented and enhanced liver CT image and feature selection was performed to select the more effected features which feature selection and reduction. Finally the selected features were used to classify the images to normal and abnormal sets using Artificial Neural Networks (ANN).

4.2 Data Acquisition:

All patients examined on a Helical Multi detector CT scanner (SOMATOM Siemens scanner dual slice, Asteion, TX-021B Toshiba scanner 16 slice , Philips Brilliance 64 slice and Aquilion ,CXXG-012A Toshiba scanner 64 slice) in Alnilein Medical Diagnostic Center, Ibn ALhythm, Dar elaj specialized hospital and Royal care international hospital respectively, used for collecting data from CT Abdominal images. With 8 second rotation Time, Large SFOV, 120kVp and 320 MA which differ through the phases.

The protocol used for Abdomen scanning triple-phase helical CT with KVp of 120 and 250 and 320 mAs, slice thickness is depending on the structure being scanned, thin data require slice thickness of 5mm for reformatted images.

Images from 41 patients were gathered. The acquisitions were performed with MDCT device and the standardized acquisition protocol was applied: helical scanning, with slice thickness 5 mm for each patient, an appropriate amount of 60% Iodinated Contrast material (about 100 -150 ml), was injected at 4 ml/s rate. The acquisition of the images in the arterial phase started about 20 seconds after contrast injection. Images corresponding to the portal phase were acquired with delay of 50–60s sequences with single Breath-holds. All images had a size of 512×512 pixels with 8-bit gray levels and were represented in DICOM format. Then all images were converted to JPG format using DICOM viewer.

4.3 Preprocessing:

Preprocessing of the liver CT image is the first step in our proposed system. Preprocessing of an image is done to reduce the noise and to enhance the image for further processing. The purpose of these steps is basically to improve the image and the image quality to get more surety and ease in the segmentation step. The contrast of the image is improved for well differentiation of the liver from its surrounding soft tissues having the same intensity level. Before applying any processing step the images are resized because they were too big to display and to have same dimension for processing purpose. Then the image was converted to gray scale because all the next steps were done on gray image. The noise removal and enhancement of contrast are done using median filter and the fine details of the image are further improved.

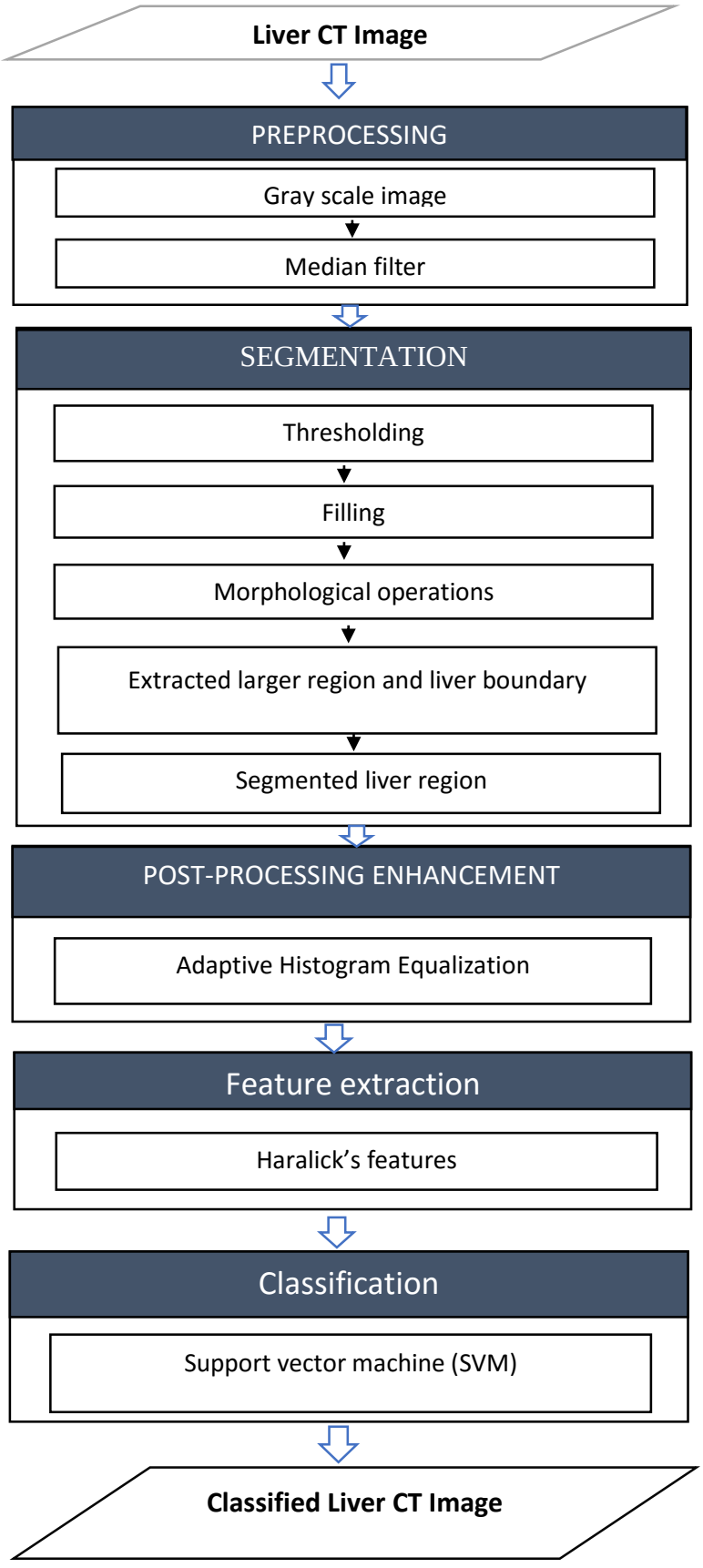

Figure 4.1: Flow chart of the proposed method

The steps of the preprocessing can be summarized as follows:

- Image resizing to 256X256.
- Image is converted to gray scale.
- A 3x3 median filter is applied on liver CT image using equation 1 in order to remove the noise.

4.3.1 Median filter:

The noise removal and enhancement of contrast are done using median filter and the fine details of the image are further improved. Median filter is a useful nonlinear digital image filtering and smoothing technique. Median filter is very effective at removing various kinds of noise as well as edge preserving. Median filter replaces the pixel value by the median value of all the pixels contained in a pre-defined neighborhood of that pixel [52], [53]. The neighborhood is usually a square window having its center at the studied pixel. The median is just the middle value of all the pixel values in the neighborhood. The Median Filter first takes all the pixel values from the surrounding neighborhood and then sorting them. The pixel with the median value is then used to replace the pixel studied. If the neighborhood under consideration having an even number of pixels, the average of the two middle pixel values is taken as a median [53].

4.4 Liver segmentation:

After enhancing the liver CT image, the next step of the proposed method is to segment the liver region from liver CT image. Segmentation is done to separate the image foreground from its background. Segmenting an image also saves the processing time for further operations which has to be applied

to the image. Global threshold is used in order to segment the liver CT image. Then some morphological operations are applied on the image to obtain the final segmented liver region. The sequence of the segmentation step was done as follows:

- Select a global threshold value for the whole CT image.
- Apply the threshold value to the preprocessed image to convert the image to binary and the thresholded image is obtained.
- Morphological close operation is applied on the thresholded image to fill in holes and small gaps in the image.
- Reserve the block whose area is the biggest and set the others to zero using 8-connected neighbors.
- The binary liver mask is obtained using the above step.
- Multiply the original liver CT image with the liver masked image to obtain the final segmented liver region with gray level values as those of original image.

4.4.1 Image Thresholding:

Image thresholding was applied as a first step in the segmentation to get binary image. Thresholding Segments image into foreground and background which called binarization of the image

$$g(x,y) \begin{cases} = 1 \text{ if } f(x,y) \text{ is foreground pixel} \\ = 0 \text{ if } f(x,y) \text{ is background pixel} \end{cases}$$

For global thresholding graythresh function on Matlab was used which computes a global threshold (level) that can be used to convert an intensity

image to a binary image with im2bw. Level is a normalized intensity value that lies in the range [0, 1].

4.4.2 Morphological operations:

After convert the image into binary image using a global thresholding anther morphological operations were done to complete the segmentation of the liver region from the abdominal image. **Morphology** is a broad set of image processing operations that process images based on shapes. Morphological operations apply a structuring element to an input image, creating an output image of the same size. In a morphological operation, the value of each pixel in the output image is based on a comparison of the corresponding pixel in the input image with its neighbors. By choosing the size and shape of the neighborhood, you can construct a morphological operation that is sensitive to specific shapes in the input image.

The most basic morphological operations are dilation and erosion. Dilation adds pixels to the boundaries of objects in an image, while erosion removes pixels on object boundaries. The number of pixels added or removed from the objects in an image depends on the size and shape of the *structuring element* used to process the image. In the morphological dilation and erosion operations, the state of any given pixel in the output image is determined by applying a rule to the corresponding pixel and its neighbors in the input image. The rule used to process the pixels defines the operation as a dilation or an erosion. Also there is another operations results from combining dilation and erosion such as morphological filling, closing and reconstruction which were used.

4.5 Post-processing:

After segmenting the liver region from liver CT image, adaptive histogram equalization is one of the post-processing techniques which applied on the segmented image. Adaptive histogram equalization is an image enhancement technique which is capable of improving the image contrast and brings out fine details of an image.

4.6. Feature extraction:

The automatic recognition and classification of biomedical objects can enhance work efficiency while identifying new inter-relationships among biological features. Feature extraction is the first step of image texture analysis in this study Haralick's features based Gray Level Co-occurrence Matrix (GLCM) are applied which calculate fourteen features were calculated as fourteenth of the features. Features obtained from this step were reduction and chose the best represented features to use for texture classification.

4.7 Feature selection and reduction:

For the selection step *ttest2* function on the matlab was used which returns a test decision for the null hypothesis that the data in two vectors array x and y comes from independent random samples from normal distributions with equal means and equal but unknown variances, using the two-sample *t*-test. The alternative hypothesis is that the data in x and y comes from populations with unequal means. The result h is 1 if the test rejects the null hypothesis at the 5% significance level, and 0 otherwise.

4.8 Image classifications:

For this step two classification methods were applied SVM and ANN then the results of them were compared to each other to choose the best one in classification of the available data and use it to design the proposed system.

4.8.1 Support Vector Machine (SVM) classification:

Firstly, the overall selected features data were putted on a matrix with dimension of 41X4 named as data, the well-known abnormal data was putted in anther matrix obtained from the first one for all column and the first 27 rows so this matrix has dimension of 27X4 named as positive, then the rest of data which is normal data was arranged in a matrix of 14X4 and named as negative. Then the supervised learning was used to learn labels by (-1) for positive data and (1) for negative data this step was followed by getting the training data to get the two classes the positive class denotes the abnormal data and the negative class denotes the normal set. To train the SVM *svmtrain* function was used, finally *svmclassify* function was used for final result prediction which returns (-1) or (1) then *msgbox* function was used to show message of classification result as abnormal if prediction returned (-1) and show normal if it returned (1).

4.8.1 Artificial Neural Network (ANN) classification:

NPRTOOL command was used to generate a MATLAB script which solves a Pattern Recognition problem with a Neural Network and it uses back propagation algorithm. In the script firstly the input and target data was defined. The input data is a matrix with dimension of **41X4** which represents the selected features, and the target data is a matrix of **2X41** and contains zeros

and ones only with respect to normal and abnormal features in the input matrix. The hidden layers were set to 20 then the network training was done using the function *train* which it's input is the created hidden layer, input data, and the target, then network was tested and its performance was found. The command *view* was used to view the network windows and finally the network was saved as check.mat.

The previous illustrated network that was created was running alt of time as training process of the network until a suitable accuracy was acquired.

CHAPTER FIVE

5. RESULTS AND DISCUSSION

This section describes and discusses the results that obtained from the applying of all the steps which illustrated before on the previous section. The sequence of all steps of the methodology was obviously discussed.

5.1 Results of image enhancement:

The results of pre-processing of image resizing to 256x256, image converting to gray scale and image enhancement using 3x3 median filter were shown in figure 5.1. The impact of the median filter was measured by the MSE and it gave an observable change.

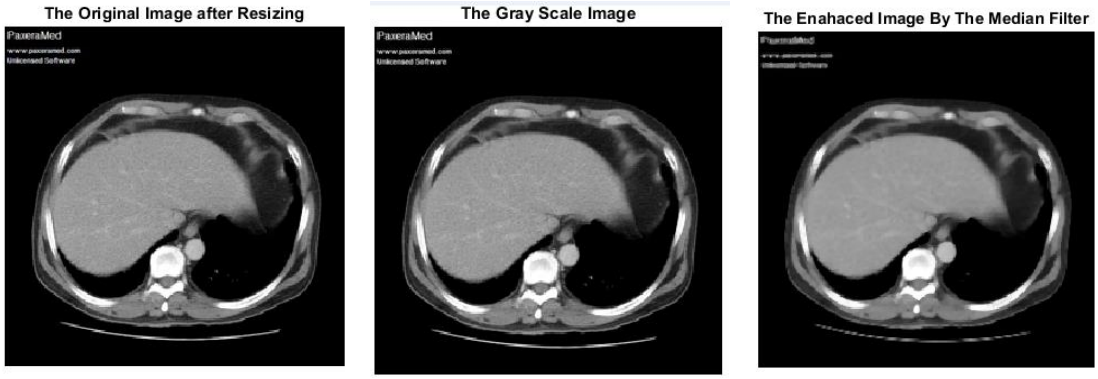

Figure 5.1: Preprocessing: a) Original Image after resizing b) gray scaled image c) median filtered image.

5.2 Results of liver segmentation:

Segmentation was done to separate the image foreground from its background. Segmenting an image also saves the processing time for further operations which has to be applied to the image. We have used segmentation using a global threshold in order to segment the liver CT image. Afterwards some morphological operations are applied on the image to obtain the final segmented liver region. The results of all segmentation steps were illustrated in figure 5.2.

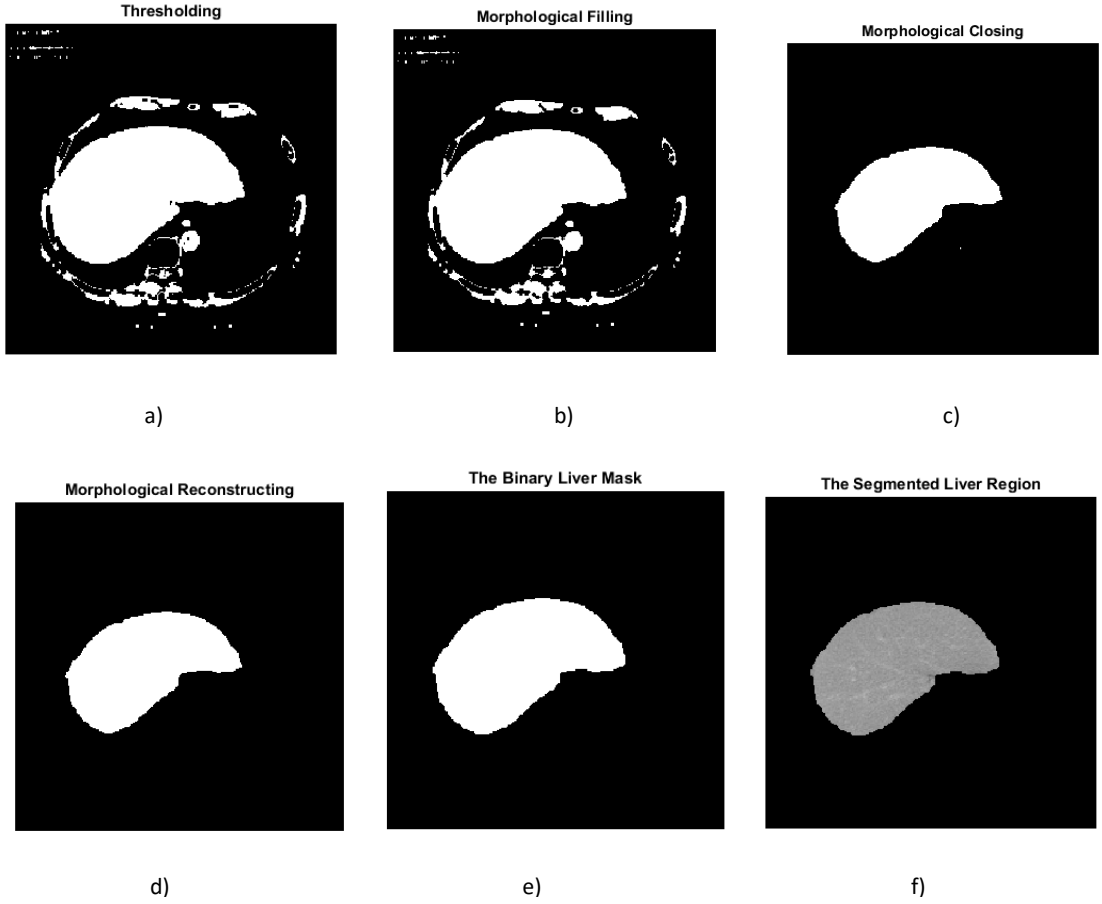

Figure 5.2: Segmentation: a) Thresholding, b) Morphological Filling, c) Morphological Closing, d) Morphological Reconstruction, e) Binary Liver Mask, f) Segmented Liver Region.

5.3 Result of post-processing:

The post-processing that was applied on the segmented liver region is the adaptive histogram equalization which improved the image contrast and fine details of an image were brought out. By visual inspection it is clear that the adaptive histogram equalized image figured out the details more than the segmented liver region which it is very useful in features extraction step because it gives a wide range from the gray intensity.

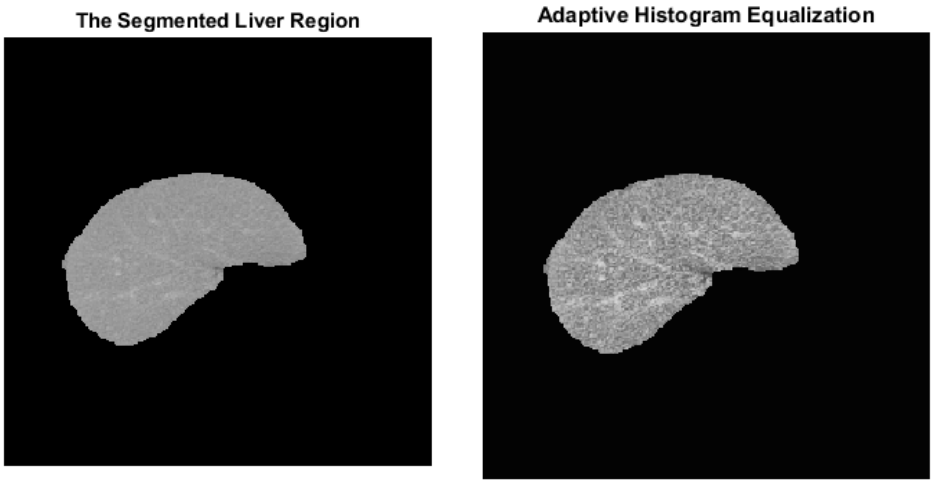

Figure5.3: post-processing: a) segmented liver region, b) Adaptive Histogram Equalization.

5.4 Results of feature extraction:

After obtaing the final image from the post_processing step 13 Haralick's featuers and variance were extracted from each image in the data sets of image cases these features were supplemented in the appendex. The features were calculated for four different angle (0°, 45°, 90°, 135°) and the mean of features geted from those angles was found. The process that follows this step is for choosing the representative data and it called features selection and reduction.

5.4.1 Features selection and reduction results:

After extracting the thirteen Haralick's featuers and the variance the result was tested to measure the degree of information they hold requierd to represent the data as normal and abnormal separate from each other. By applying the *ttest2* function to all features in all directions (0°, 45°, 90°, 135°) and from their mean, the angle of 90° gave the large numbers of representative features which are four features that were found they effective on differentiation between the normal and abnormal data from all the data sets, those features are: **Contrast, Correlation, Difference Average, and Difference Variance.** The result of applying *ttest2* function were illustrated in table 2.

Also the relation between each feature to all the data set was plotted as shon in figure 5.4 from(5.4.a to 5.4.n) crosponding to features in table 2 from (1 to 14). For all the graphs in fingure 5.4 the x-axis represents the number of the data set from (1 to 41) which the first numbers until 27 represent the abnormal data and the rest represent the normal data. The plots were found to all the angles and also for the mean of them and the best representative angle was 90°, so here only the plots of this angle were provided and the others were not supplemented they just had used for compression between the visual selection from the graphical figures and the result from using *ttest2* function, and it's clear that it's difficult to select the features visually. So the four features which were selected is according to the result of *ttest2* function just.

Those features which were selected consider as the input for the classification step. From the previous discussion the dimension of the matrix of features that will be input for the classification is **41X4.** This matrix was selected from the

features table of angle 90° in the appendix and elements of it were highlighted on that table as column 2, 5, 12, and 13 with respect to all rows.

Table 2: Feature Selection using ttest2 function of angle 90°

NO.	Features	a0	a45	a90	a135
1.	Energy	0	0	0	0
2.	Contrast	1	1	1	1
3.	Entropy	0	0	0	0
4.	Inverse_diff	0	0	0	0
5.	Correlation	0	0	1	0
6.	Info_corr_1	0	0	0	0
7.	Info_corr_2	0	0	0	0
8.	Sum_var	0	0	0	0
9.	Sum_entropy	0	0	0	0
10.	Sum_avg	0	0	0	0
11.	Variance	0	0	0	0
12.	Diff_avg	1	1	1	1
13.	Diff_var	1	1	1	1
14.	Diff_entropy	0	0	0	0

Figure 5.4: illustrates the graphical technique of features selection process from angle 90° of Haralick's features it contains 14 graphs for all the features calculated, **a)** for **energy**, **b)** for **contrast**, **c)**, for **Entropy**, **d)** for **Inverse difference**, **e)** for **Correlation**, **f)** for **Information measure of correlation 1**, **g)** for **Information measure of correlation 2**, **h)** for **Sum Variance**, **i)** for

Sum entropy, **j)** for **Sum average**, **k)** for **Variance**, **l)** for **Difference average**, **m)** for **Difference variance**, and **n)** for **Difference entropy**.

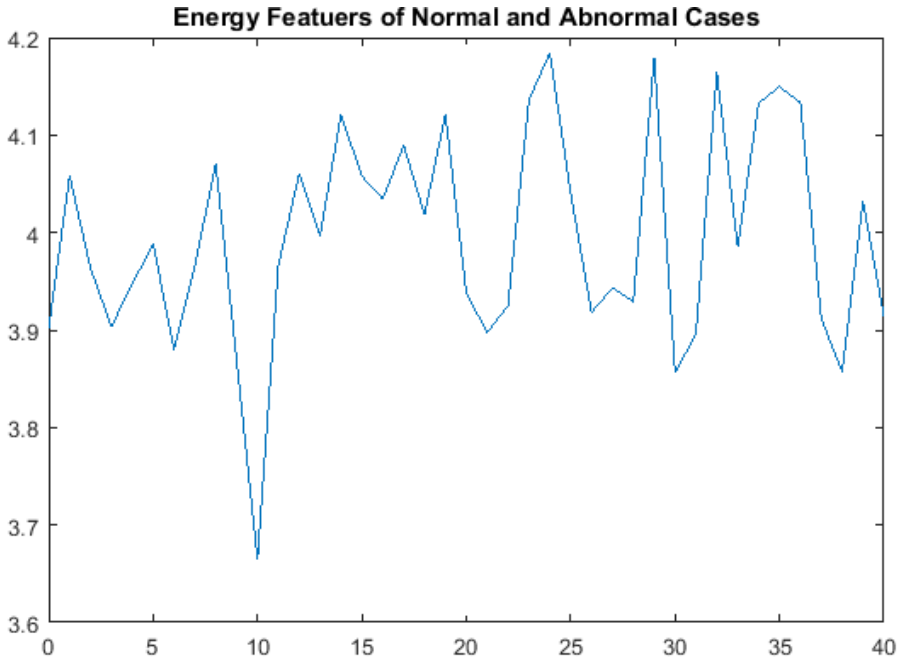

Figure 5.4.a: Energy features of normal and abnormal cases.

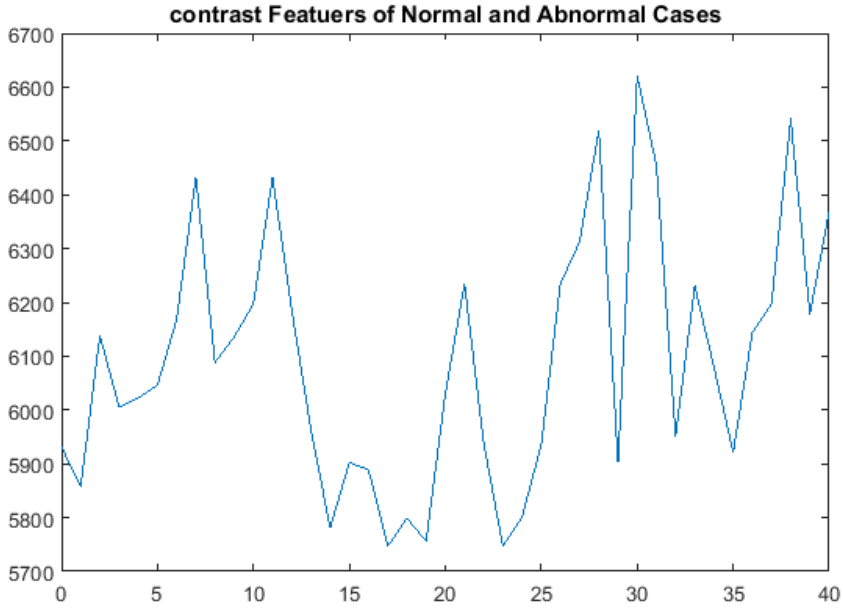

Figure5.4. b: Contrast features of normal and abnormal cases.

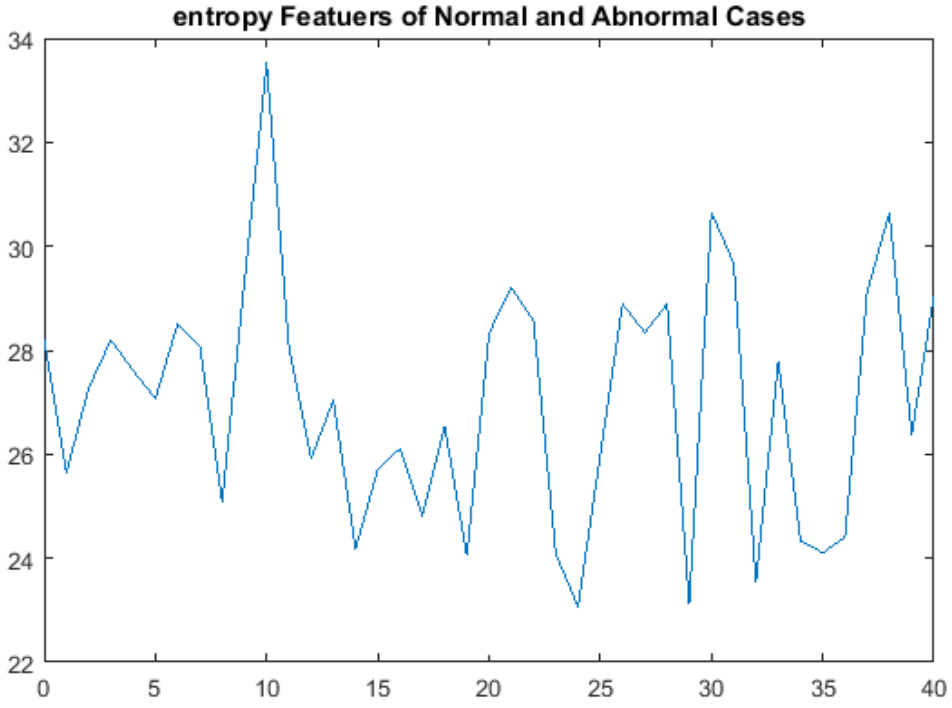

Figure 5.4.c: Entropy features of normal and abnormal cases.

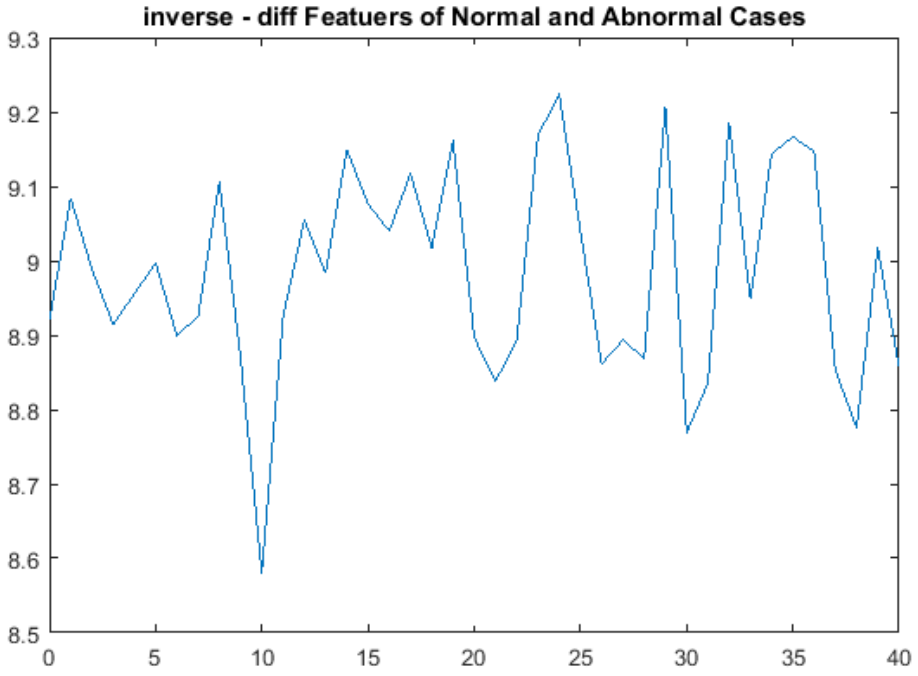

Figure 5.4.d: Inverse difference features of normal and abnormal cases.

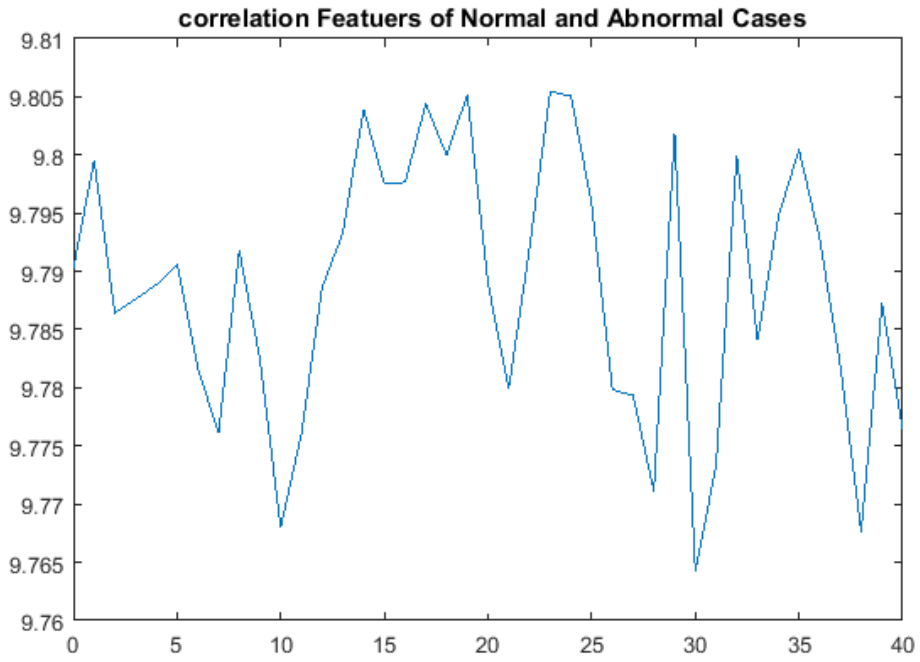

Figure 5.4.e: Correlation features of normal and abnormal cases.

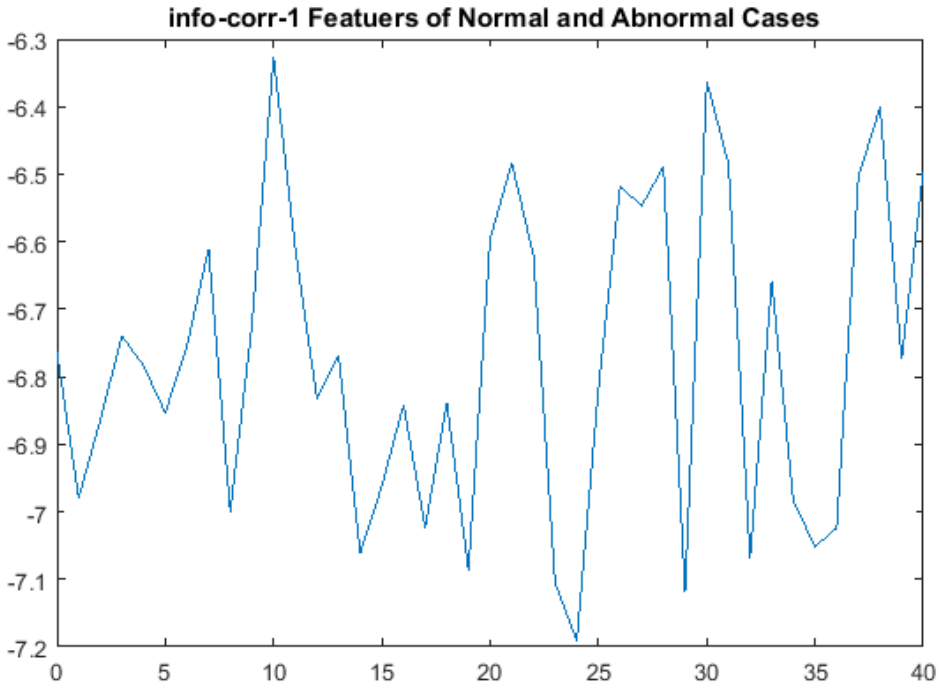

Figure 5.4.f: information measure of correlation 1 features of normal and abnormal cases.

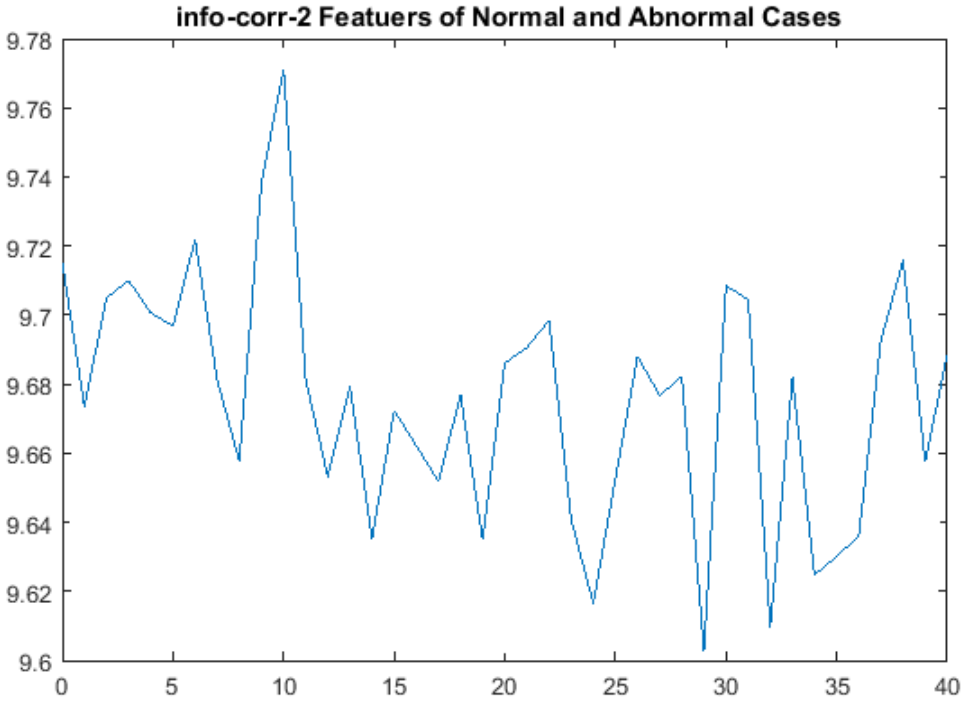

Figure 5.4.g: Information measure of correlation 2 features of normal and abnormal cases.

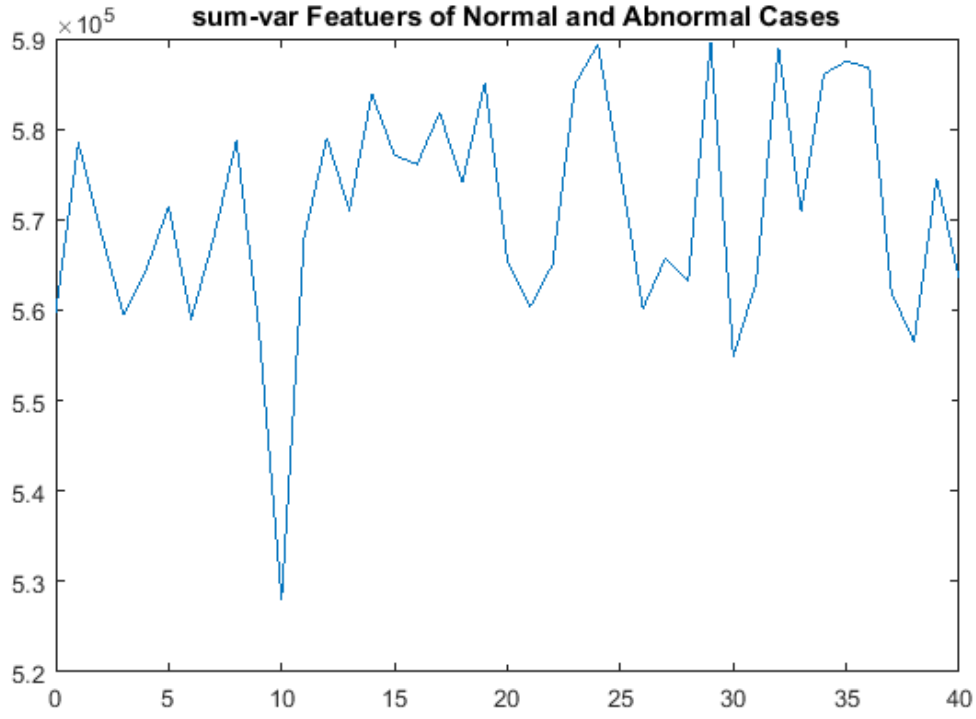

Figure 5.4.h: Sum variance features of normal and abnormal cases.

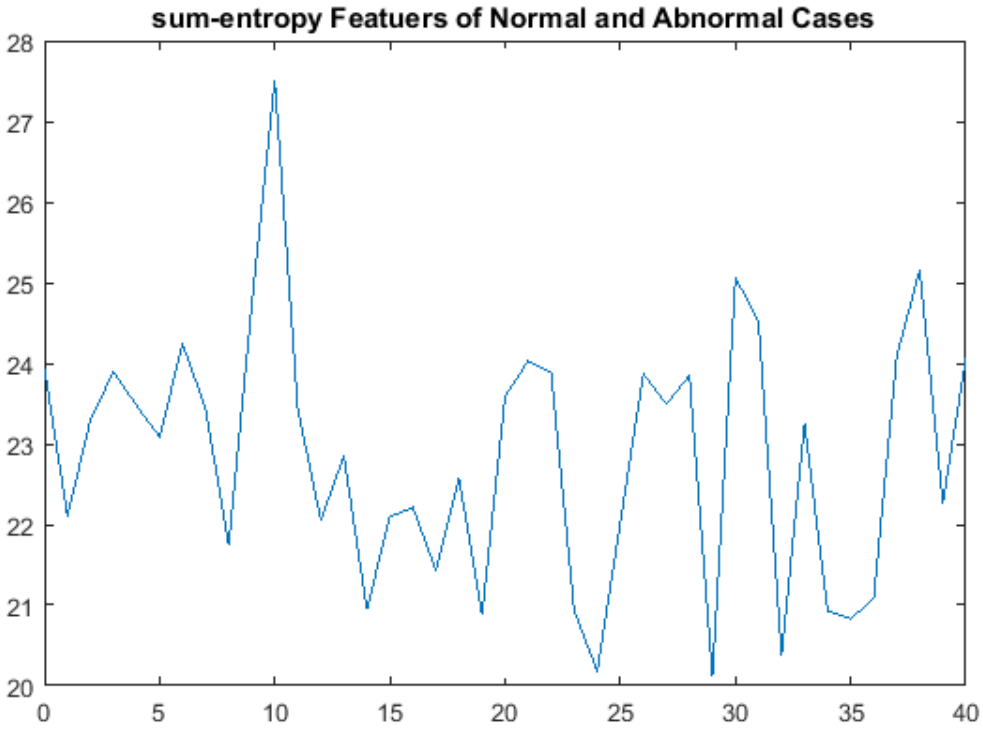

Figure 5.4.i: Sum entropy features of normal and abnormal cases.

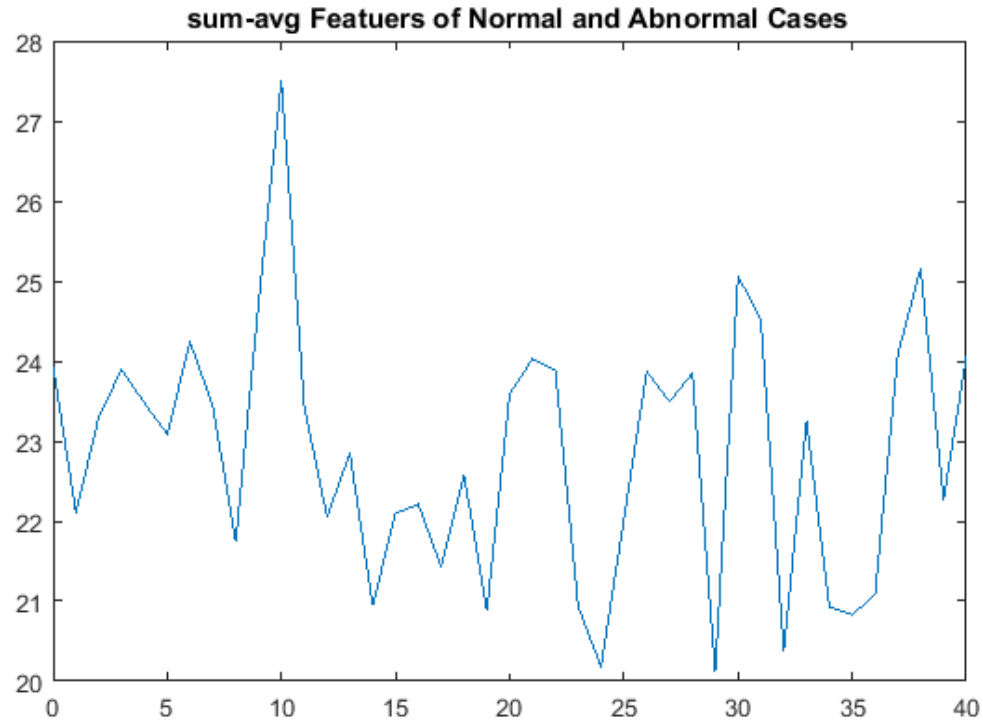

Figure 5.4.j: Sum average features of normal and abnormal cases.

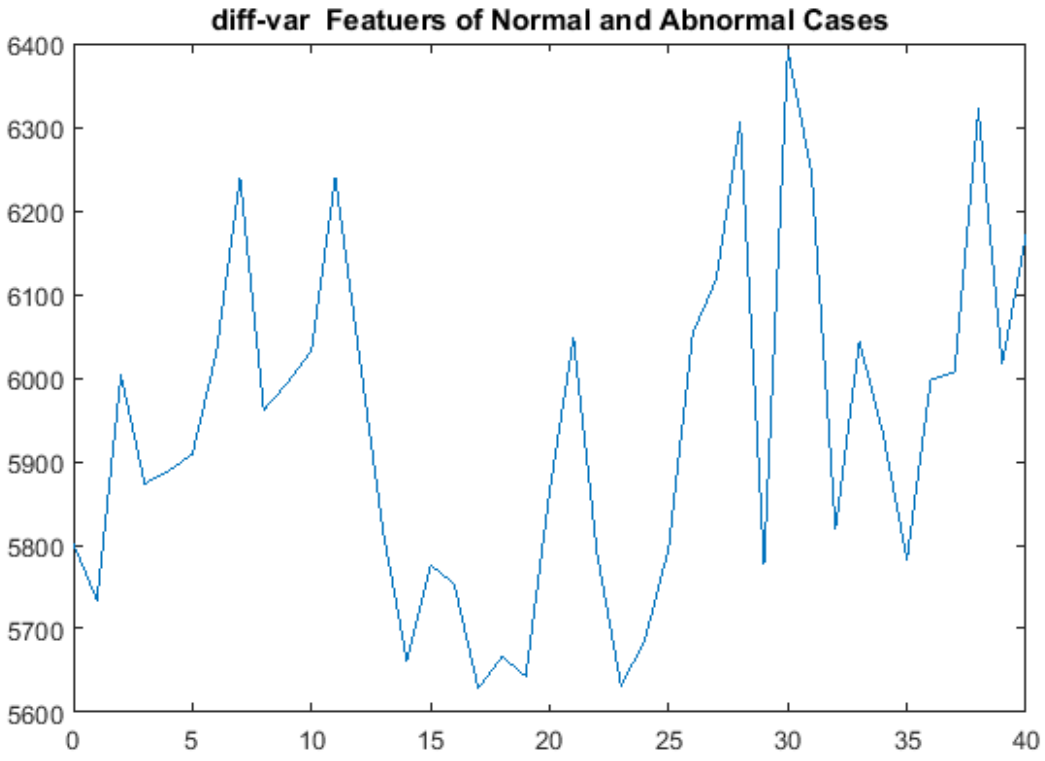

Figure 5.4.k: difference variance features of normal and abnormal cases.

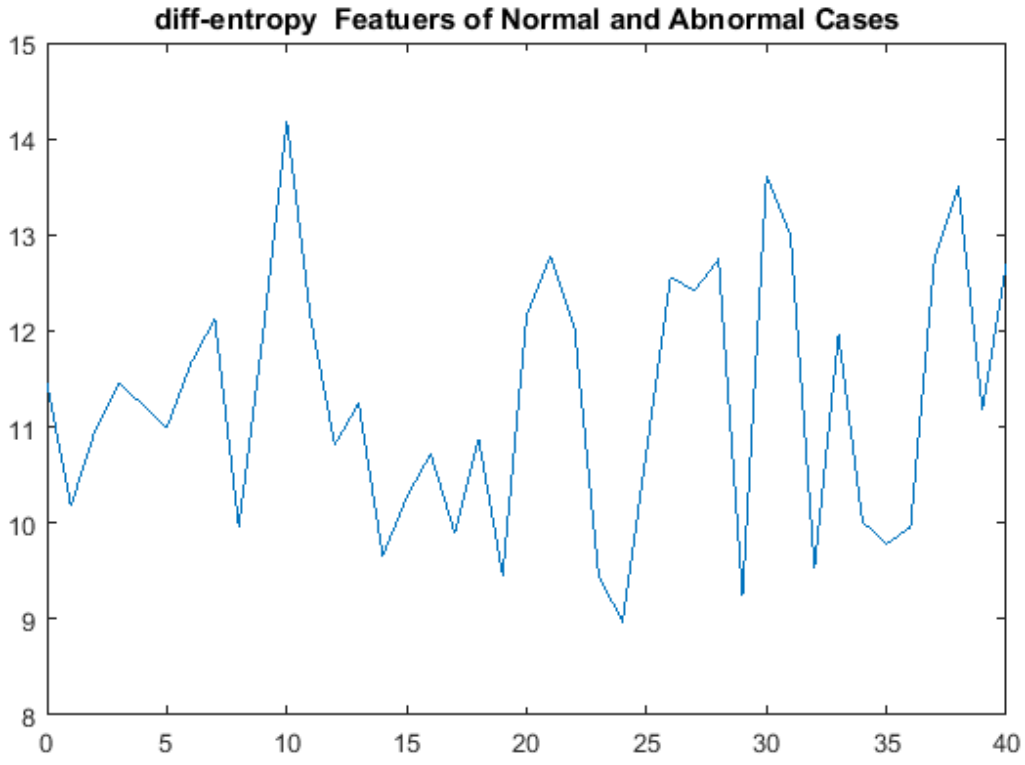

Figure 5.4.l: difference entropy features of normal and abnormal cases.

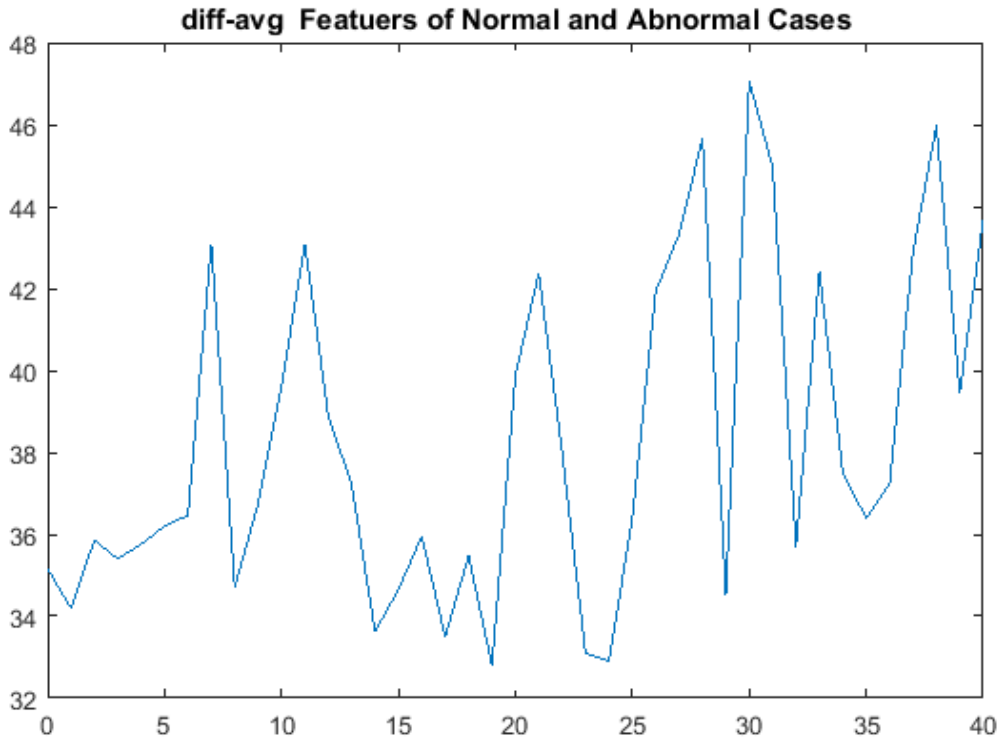

Figure 5.4.m: difference average features of normal and abnormal cases.

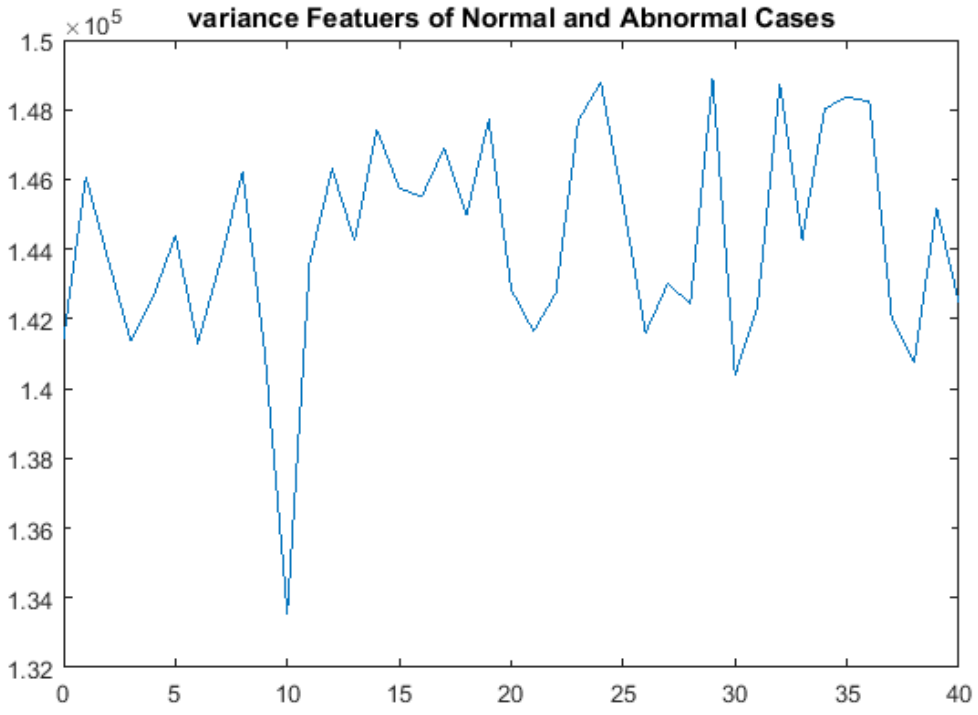

Figure 5.4.n: Variance features of normal and abnormal cases.

5.5 Results of image classification:

Features that selected to represent the data as normal and abnormal. For classification both of SVM and ANN classification techniques were used and the accuracy and performance of each of them were calculated.

The selected features from the previous step were used as input to classification step. Both of the SVM and ANN show those massages which illustrated in figure 5.5.1 as final result of the classification step.

a) b)

Figure 5.5.1: classification result: a) for abnormal and b) for normal data.

For ANN additional windows and graphs appear when running it which clarify the architecture of the network that was created. Two windows are opening immediately after running the created network the first one is the neural network training which illustrates the neural network architecture, algorithm that used, progress, and plots that can show. The next window that will next appears is the pattern recognition neural network architecture, in this case there are two input set to get two output set also (normal and abnormal), and the hidden layers were set to be 20 layers as recommended in the literature. Then from the neural network window four figures were plotted by

checking in their icon which are: performance, training state, error histogram, and confusion matrix.

Figure 5.5.2: shows the running of network: a) **Neural Network Training**, b) **Neural Network Architecture,** c) **Performance,** d) **Training State**, e) **Error Histogram**, and f) **Confusion Matrix**.

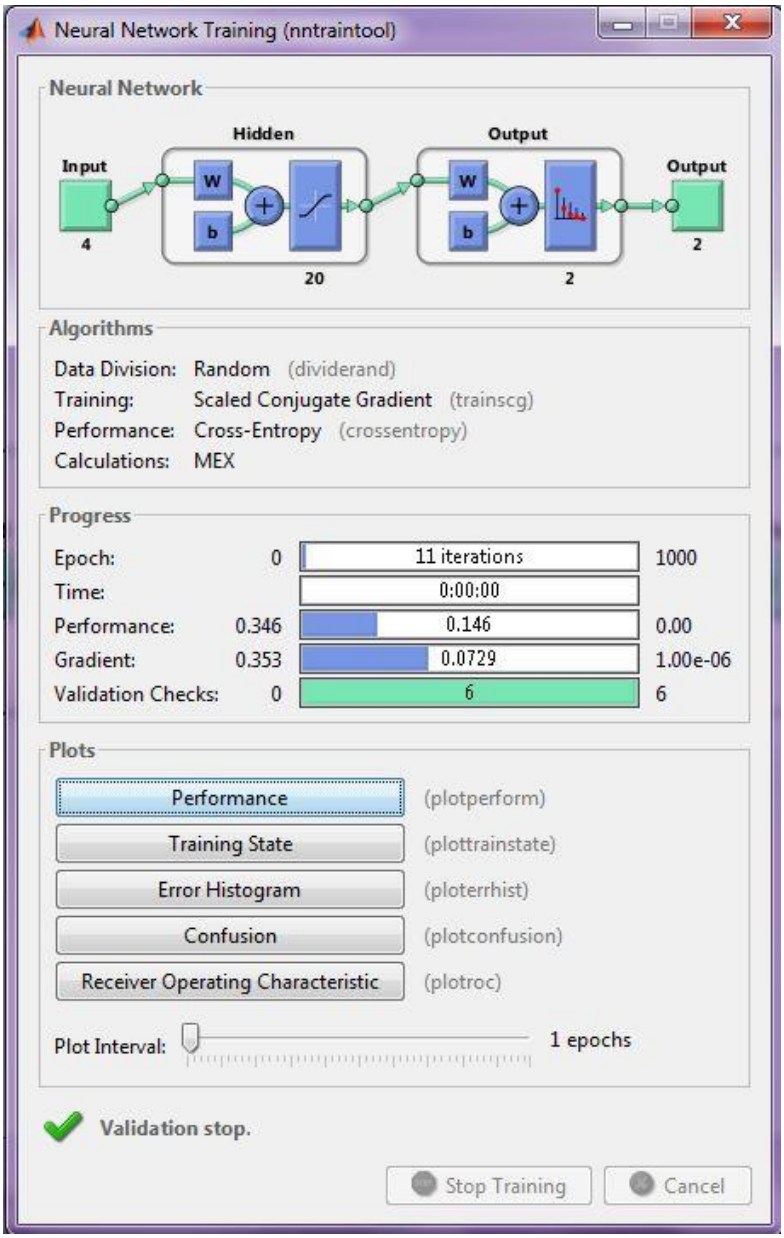

Figure 5.5.2.a: Neural Network Training

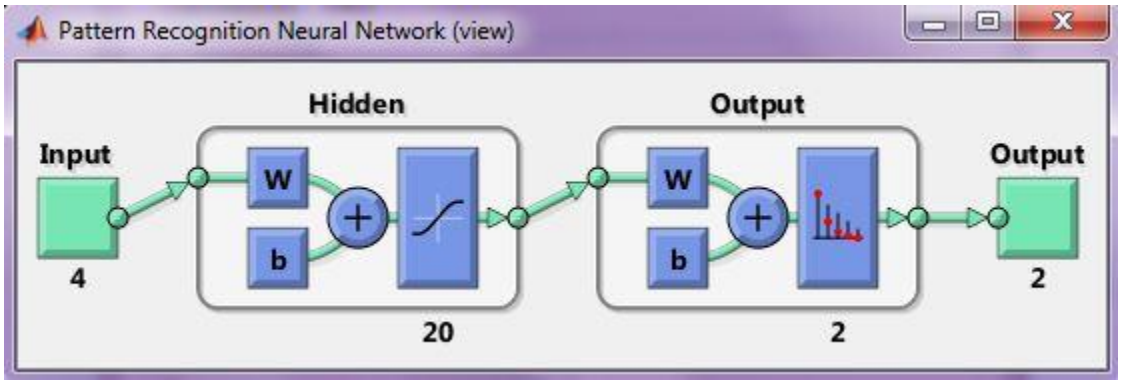

Figure 5.5.2.b: Neural Network Architecture

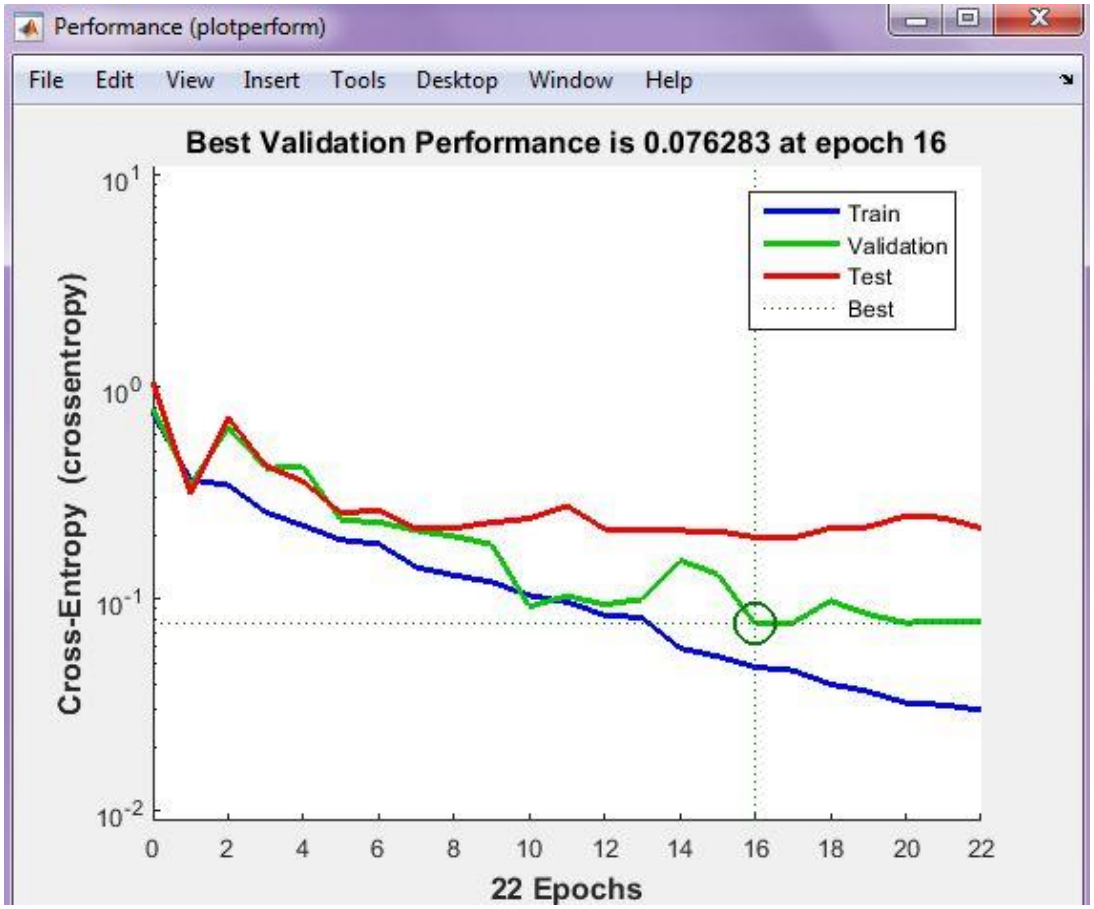

Figure 5.5.2.c: Performance

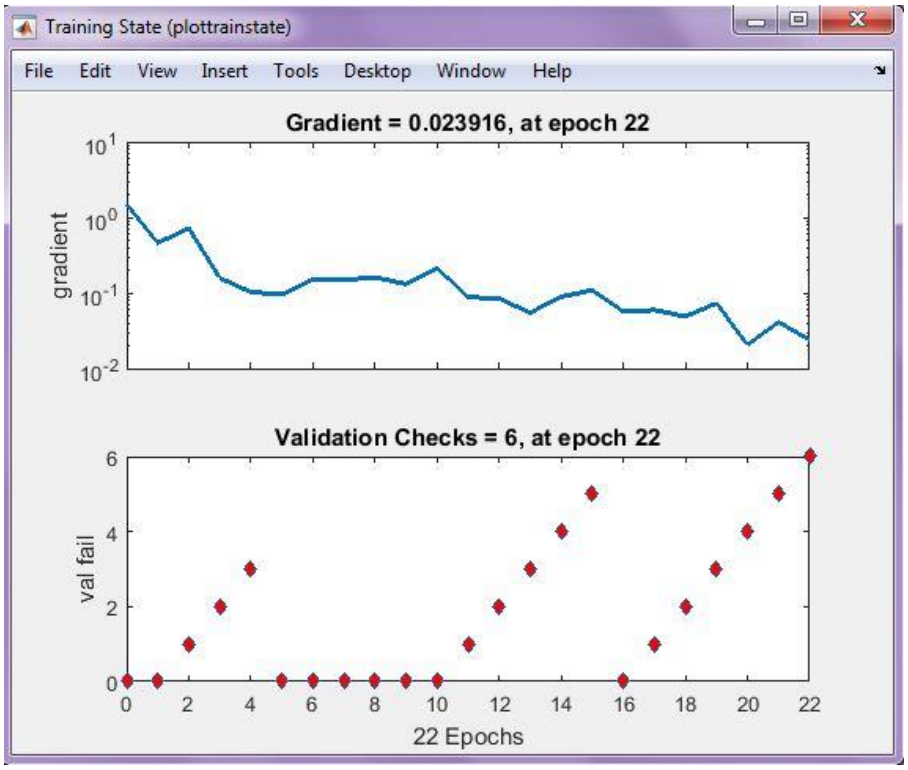

Figure 5.5.2.d: Training State

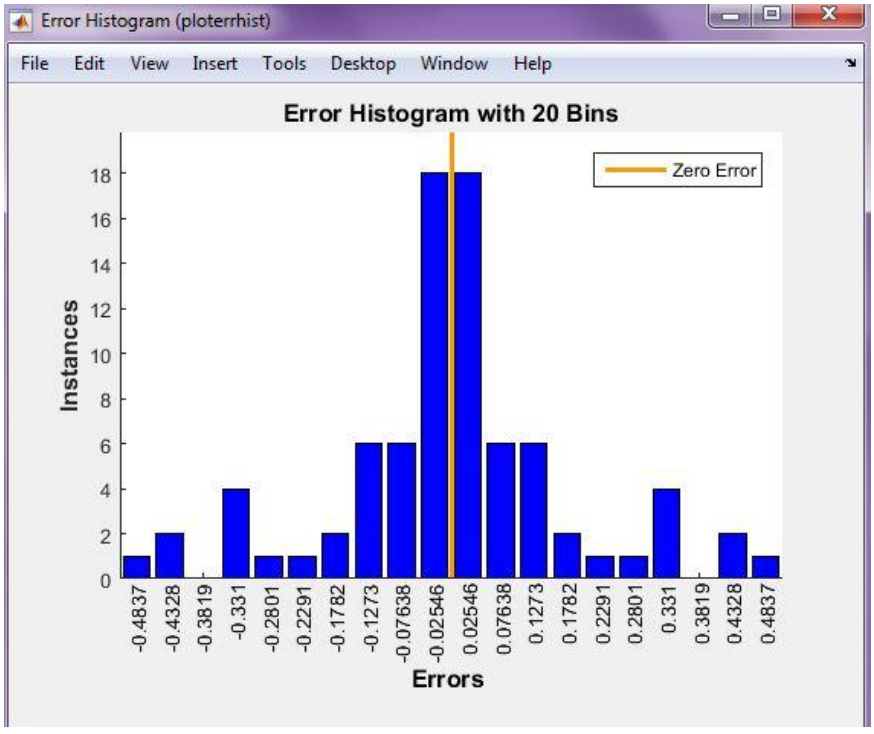

Figure 3.5.2.e: Error Histogram

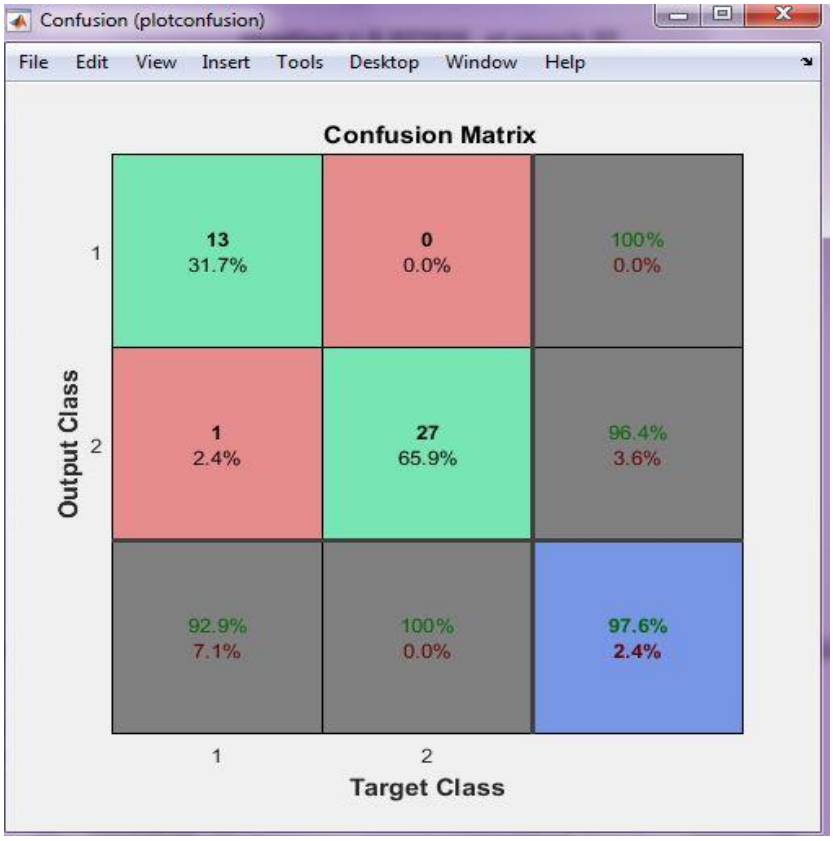

Figure 5.5.2.f: Confusion Matrix

5.5.1 Performance Evaluation of Classification:

The performance of both classification methods was calculated using the below statistical terms:

A true positive (TP): Results when a test indicates a positive status when the true status is also positive.

A true negative (TN): Results when a test indicates a negative status when the true status is also negative.

A false positive (FP): Results when a test indicates a positive status when the true status is negative.

A false negative (FN): Results when a test indicates a negative status when the true status is positive.

The sensitivity of a test (or symptom): Is the probability of a positive test result (or presence of the symptom) given the presence of the disease.

$$\text{Sensitivity} = \frac{\text{TP}}{\text{TP} + \text{FP}} \times 100 \ldots\ldots\ldots\ldots\ldots\ldots\ldots\ldots 18$$

The specificity of a test (or symptom): Is the probability of a negative test result (or absence of the symptom) given the absence of the disease.

$$\text{specificiity} = \frac{\text{TN}}{\text{TN} + \text{FN}} \times 100 \ldots\ldots\ldots\ldots\ldots\ldots\ldots\ldots 19$$

Accuracy: Accuracy is how close a measured value is to the actual (true) value.

$$\text{Accuracy} = \frac{\text{Number of Correct Data}}{\text{Number of All Data}} \times 100 = \frac{\text{TP+TN}}{\text{TOTAL}} \text{X } 100 \ldots\ldots\ldots\ldots\ldots 20$$

The performance of SVM was illustrated in table 3, then sensitivity, specificity, and accuracy of it were calculated.

Table 3: performance evaluation of SVM classification:

Test Result / **True Status**	**Abnormal**	**Normal**	**Total**
Positive	22 (TP)	0 (FN)	**22**
Negative	5 (FP)	14 (TN)	**19**
Total	**27**	**14**	**41**

From table 3, **TP = 22, FP = 5, FN = 0, TN =14, Total = 41**, and by applying in the above equation:

$$\text{Sensitivity } = \frac{22}{22+5} \times 100 = 81.48\ \%$$

$$\text{specificiity } = \frac{14}{14+0} \times 100 = 100\ \%$$

$$\text{Accuracy} = \frac{22+14}{41}\ \text{X}\ 100 = 87.80\ \%$$

The performance of ANN was illustrated in table 4, and same as for SVM also sensitivity, specificity, and accuracy of it were calculated. The performance evaluation table of ANN is same as the confusion matrix shown in figure 5.5.2.f.

Table 4: performance evaluation of ANN classification:

Test Result / **True Status**	**Abnormal**	**Normal**	**Total**
Positive	27 (TP)	1 (FP)	**28**
Negative	0 (FP)	13 (FN)	**13**
Total	**27**	**14**	**41**

For table 4, **TP = 27, FP = 0, TN =13, FN = 1, and Total = 41**

$$\text{Sensitivity } = \frac{27}{27+0} \times 100 = 100\ \%$$

$$\text{specificiity } = \frac{13}{13+1} \times 100 = 92.86\%$$

$$\text{Accuracy} = \frac{27+13}{41} \text{ X } 100 = 97.56\ \%$$

It's clear that from the performance evaluation both of the SVM and ANN the accuracy of SVM is (87.80 %) while of ANN is (97.56 %) which means artificial neural network gave more accurate result for the data used in this study. So for final classification step ANN classification method was chosen and applied in the proposed system.

CHAPTER SIX

6. CONCLUSION AND RECOMMENDATION

6.1 Conclusion:

The aim of this study is to design and improve an automated system for liver classification as normal or abnormal to help physicians in their diagnosis and treatment plan. The data has been collected for this study from different specialized CT center then it has been processed in different step from converting its format to suitable format until enhancing the contrast of the image. An automatic segmentation of liver region after applying different enhancement techniques has been performed, then the features have been extracted from the segmented liver region using Haralick's feature, this step has followed by features selection and reduction to choose the best representative features. As final step selected features has been classified into two classes normal or abnormal. Artificial Neural Network (ANN) and Support Vector Machine has been applied in the classification step. The performance of each classification methods has been calculated and found that SVM has accuracy 87.80 % and sensitivity 81.48 % and ANN has accuracy 97.56 % and sensitivity 100 %.

So it can be concluded that the Artificial Neural Network is suitable for the data was used, and it has been used for the classification step in the proposed system.

6.2 Recommendation and future work:

- Increase the number of samples to get more accurate result.
- Perform additional enhancement techniques such as edge detection to make the segmentation step easier than the proposed one.
- Try another segmentation technique which can avoid the segmentation drawback in this study.
- Apply a lot of effort to extract the tumor region after extracting the overall liver region for more accurate features.
- Try another features extracting techniques and compare the result of classification step with the result that was provided here.
- Design a Graphical User Interface (GUI) system to perform all the steps in an easy manner.

References:

[1] Chen, Y., Yi, Q., and Mao, Y., "Cluster of liver cancer and immigration: A geographic analysis of incidence data for ontario 1998-2002," International Journal of Health Geographics, vol. 7, no. 28, pp. 1-17, 2008.

[2] R.Rajagopal, P.Subbiah, "Computer Aided Detection of Liver Tumor using SVM Classifier" Research Scholar, Dept. of ECE, St. Peter University, Avadi, Chennai, Tamilnadu, India1, Principal, Bharath College of Engg. & Tech. for Women, Kadapa, Andhra Pradesh 516 003, India2, Vol. 3, Issue 6, June 2014.

[3] M. Usman Akram, Aasia Khanum and Khalid Iqbal, " An automated System for Liver CT Enhancement and Segmentation" Department of Computer Engineering, College of Electrical and Mechanical Engineering, National University of Sciences and Technology, Pakistan, ICGST-GVIP Journal, Volume 10, Issue IV, October 2010.

[4] Dr. Ahmet Gurakar, Ahmet Gurakar, M.D, James P. Hamilton, M.D, Ayman Koteish, M.D, Zhiping Li, M.D, Esteban Mezey, M.D, Hepatocellular Carcinoma (Liver Cancer).

[5] American Cancer Society. Cancer Facts & Figures 2016. Atlanta, Ga: American Cancer Society; 2016.

[6] American Joint Committee on Cancer. Liver. In: AJCC Cancer Staging Manual. 7th ed. New York, NY: Springer; 2010.

[7] Fong,Y, Dupey,DE,, Feng M, Abou-Alfa G. Cancer of the liver. In: DeVita VT, Lawrence TS, Rosenberg SA, eds. DeVita, Hellman, and Rosenberg's Cancer: Principles and Practice of Oncology. 10th ed. Philadelphia, Pa: Lippincott Williams & Wilkins; 2015.

[8] Brandi G, de Rosa F, Agostini V, et al. Metronomic capecitabine in advanced hepatocellular carcinoma patients: a phase II study. Oncologist. 2013; 18(12):1256 7. Epub 2013 Nov 13.

[9] Bruix J, Sherman M. Management of hepatocellular carcinoma. Hepatology. 2005.

[10] Ben Ariff, Claire R Lloyd, Sameer Khan, Mohamed Shariff, Andrew V Thillainayagam, Devinder S Bansi, Shahid A Khan, Simon D Taylor-Robinson, Adrian KP Lim, 'Imaging of liver cancer' World J Gastroenterol 2009 March 21; 15(11): 1289-1300.

[11] Ryder SD. Guidelines for the diagnosis and treatment of hepatocellular carcinoma (HCC) in adults. Gut 2003; 52 Suppl 3: iii1-iii8.

[12] Khan SA, Davidson BR, Goldin R, Pereira SP, Rosenberg WM, Taylor-Robinson SD, Thillainayagam AV, Thomas HC, Thursz MR, Wasan H. Guidelines for the diagnosis and treatment of cholangiocarcinoma: consensus document. Gut 2002; 51 Suppl 6: VI1-VI9.
[13] Cosgrove DO, Eckersley R. Contrast-enhanced ultrasound: Basic physics and technology overview. In: Lencioni R. Enhancing the role of ultrasound with ultrasound contrast agents. Pisa: Springer, 2006: 3-14.
[14] Kono Y, Steinbach GC, Peterson T, Schmid-Schonbein GW, Mattrey RF. Mechanism of parenchymal enhancement of the liver with a microbubble-based US contrast medium: an intravital microscopy study in rats. Radiology 2002; 224: 253-257.
[15] Yanagisawa K, Moriyasu F, Miyahara T, Yuki M, Iijima H.Phagocytosis of ultrasound contrast agent microbubbles by Kupffer cells. Ultrasound Med Biol 2007; 33: 318-325
[16] Weg N, Scheer MR, Gabor MP. Liver lesions: improved detection with dual-detector-array CT and routine 2.5-mm thin collimation. Radiology 1998; 209: 417-426
[17] Foley WD, Mallisee TA, Hohenwalter MD, Wilson CR, Quiroz FA, Taylor AJ. Multiphase hepatic CT with a multirow detector CT scanner. AJR Am J Roentgenol 2000; 175: 679-685
[18]Glockner JF. Hepatobiliary MRI: current concepts and controversies. J Magn Reson Imaging 2007; 25: 681-695 14
[19] Teefey SA, Hildeboldt CC, Dehdashti F, Siegel BA, Peters MG, Heiken JP, Brown JJ, McFarland EG, Middleton WD, Balfe DM, Ritter JH. Detection of primary hepatic malignancy in liver transplant candidates: prospective comparison of CT, MR imaging, US, and PET. Radiology 2003; 226: 533-542
[20] Semelka RC, Helmberger TK. Contrast agents for MR imaging of the liver. Radiology 2001; 218: 27-38
[21] Gandhi SN, Brown MA, Wong JG, Aguirre DA, Sirlin CB. MR contrast agents for liver imaging: what, when, how. Radiographics 2006; 26: 1621-1636
[22] Meikle SR, Dahlbom M. Positron emission tomography (PET). In: Ell PJ, Gambhir SS. Nuclear medicine in clinical diagnosis and treatment. Edinburgh: Churchill Livingstone, 2004: 1827-1843
[23] Choi BY, Nguyen MH. The diagnosis and management of benign hepatic tumors. J Clin Gastroenterol 2005; 39: 401-412

[24] Lawrence Pan, MS IV, 'Common CT Findings Secondary to Liver Tumors' New Jersey Medical School Radiology – Beth Israel Deaconess Medical Center September 2006

[25] Digital Image Processing - A Remote Sensing Perspective, Jhon R. Jenson, 3rd Edition, Prentice – Hall, 2003.

[26] Bankman IN (ed). Handbook of Medical Image Processing and Analysis. 2nd ed. New York: Academic Press; 2008. ISBN: 0-123-73904-7

[27] M. C. Nicolae, L. Moraru and L. Onose "Comparative Approach for Speckle Reduction in
Medical Ultrasound Images," Romanian J. Biophys., Vol. 20, No. 1, pp. 13–21, Bucharest, 2010.

[28] R. Sivakumar and D. Nedumaran, "Comparative study of Speckle Noise Reduction of Ultrasound Bscan Images in Matrix Laboratory Environment," International Journal of Computer Applications (0975-8887), Vol. 10, No. 9, November 2010.

[29] R. Vanithamani and G. Umamaheswari, "Performance Analysis of Filters for Speckle Reduction in Medical Ultrasound Images," International Journal of Computer Applications (0975-8887), Vol. 12, No. 6, December 2010.

[30] Haralick, Robert M., and Linda G. Shapiro, Computer and Robot Vision, Volume I. Addison-Wesley, 1992.

[31] Sonka. M, Hlavac. V, Boyle. R, Image Processing, Analysis and Machine Vision, PWS Publishing, 1998.

[32] P. Venkatesan and G. Nagarajan, "Non Linear Algorithm for Removal of Mixed Gaussian Noise and Impulse Noise Using Fuzzy Filters", ICCCI 2011, January 11-12, 2011.

[33] Zhang Lei, Song Hongxun, "A Hybrid Filter based on an adaptive neuro - fuzzy inference system for efficient removal of impulse noise from corrupted digital images", IEEE 2nd Conference on Environmental Science and Information Application Technology, 2010.

[34] P.Deepa and M.Suganthi, Department of Computer Science and Engineering Muthayammal Engineering College, Rasipuram, 'Performance Evaluation of Various Denoising Filters for Medical Image' P.Deepa et al, / (IJCSIT) International Journal of Computer Science and Information Technologies, Vol. 5 (3) , 2014, 4205-4209.

[35] BUI Dinh Tien and Dr. HUYNH Trung Hieu, UNIVERSITY OF BORDEAUX 1, Studying methods of automatic liver segmentation from MRI images, January 15, 2015.
1, Jan-Feb 2010.
[36] Haralick, R.M., Shanmugam, K., and Dinstein, Its'Hak, "Textural Features for Image Classification," Systems, Man and Cybernetics, IEEE Transactions, vol.SMC-3, no.6, pp.610,621, Nov. 1973.
[37] Jensen, J.R. 1996. Introduction to Digital Image Processing: A Remote Sensing Perspective.
Practice Hall, New Jersey.
[38] QeetharaKadhim Al-Shayea "Artificial Neural Networks in Medical Diagnosis," IJCSI International Journal of Computer Science Issues, vol. 8, 2011.
[39] E. Boser, I. Guyon, and V. Vapnik. A training algorithm for optimal margin classi_ers. In Proceedings of the Fifth Annual Workshop on Computational Learning Theory, pages 144{152. ACM Press, 1992.
[40] Cortes and V. Vapnik. Support-vector network. Machine Learning, 20:273{297, 1995}
[41] A.H. Mir, M. Hanmandlu, and S.N. Tandon, “Texture analysis of CT images,” IEEE Engineering in Medicine and Biology, 1995.
[42] K. Mala, and V. Sadasivam, “Automatic segmentation and classification of diffused liver diseases using wavelet based texture analysis and Neural Network,” IEEE Indicon Conference, pp. 216-219, 2005.
[43] V.S. Bharathi, M.A.L. Vijilious, and L.Ganesan, “Orthogonal Moments based texture analysis of CT liver images,” International Conference on Computational Intelligence and Multimedia Applications, 2007.
[44] Luo et al., “Automatic liver parenchyma segmentation from abdominal CT images using Support Vector Machines” IEEE, 2009.
[45] Mallat, S., “Multifrequency channel decomposition of images and wavelet models,” IEEE Trans. Acoustic, Speech and Signal Processing,
pp. 2091-2110, 1989.
[46] Rosenfeld, A., and Weszka, J., “Picture recognition in digital pattern recognition,” K. Fu (Ed.), Springer-Verlag, pp. 135-166, 1980.

[47] Daugman, J., "Uncertainty relation for resolution in space, spatial frequency and orientation optimised by 2-Dimensional visual cortical filters," Journal of the Optical Society of America, pp. 1160-1169, 1985.

[48] K. Wu, C. Garnier, J. Louis, Coatrieux, and H. Shu, "A preliminary study of moment-based texture analysis for medical images" 32nd Annual International Conference of the IEEE EMBS, 2010.

[49] Ismail Ben Ayed, Member, IEEE, and Amar Mitiche, Member, IEEE "A Region Merging Prior for Variational Level Set Image Segmentation", IEEE transactions on image processing, vol. 17, no. 12, December 2008.

[50] Kasparis T., Tzannes N. S, Bassiouni M. and Chen Q. Department of Electrical and Computer Engineering and 2Department of Computer Science, University of Central Florida, Orlando, FL 32816, U.S.A."Texture description using fractal and Energy features" Computers Elect. Engng Vol.21, No. I, pp. 21-32, 1995.

[51] Lundahl T., Ohley W. J., Kay S. M., and Siffert R., "Fractional Brownian motion: A maximum likelihood estimator and its application to image texture," IEEE Trans. Med. Imag., vol. MI-5, pp. 152–161, 1986.

[52]. kumar,KUntal, Chowdhury, "Image Enhancement Using Guided Image Filter Technique" International Journal of Engineering and Advanced Technology (IJEAT) ISSN : 2249 – 8958, Volume-1, Issue-5, June 2012.

[53] Smriti Sahu 1, Maheedhar Dubey2, Mohammad Imroze Khan3, Jitendra Kumar 4,' Comparative Evaluation of Filters for Liver Ultrasound Image Enhancement' Department of Electronics & Telecommunication Engineering, Chhatrapati Shivaji Institute of Technology, Durg, C.G., (India) Volume 2, Issue 1, January – February 2013.

Appendix

This section contains the fourteen calculated features of Haralick's feature extraction for the four angle (90°) and for the mean of those angle. Also it contains the four selected features

energy	contrast	entropy	inverse_diff	correlation	info_corr_1	info_corr_2	sum_var	sum_entropy	sum_avg	variance	diff_avg	diff_var	diff_entropy
0.39639	441.0834	2.75870	0.898742	0.984396	-0.70476	0.974843	56093.75	2.356898	306.2249	14133.71	2.841625	433.0085	1.072861
0.41191	441.4024	2.50955	0.913822	0.984884	-0.7243	0.970637	57961.59	2.175286	301.107	14600.75	2.805236	433.5331	0.954971
0.40260	458.4971	2.66165	0.905832	0.984038	-0.71634	0.974027	56988.55	2.291469	303.9183	14361.76	2.881555	450.1937	1.017844
0.39644	449.9139	2.75320	0.898432	0.984079	-0.70379	0.974526	56069.98	2.352522	306.6668	14129.97	2.859263	441.7385	1.069337
0.40084	449.5925	2.69832	0.901916	0.984229	-0.70698	0.973498	56564.72	2.309938	305.9439	14253.58	2.88747	441.255	1.05105
0.40497	454.4016	2.65047	0.904933	0.984255	-0.71116	0.972798	57267.22	2.270901	304.3602	14430.4	2.957159	445.6568	1.033695
0.3942	458.8972	2.78654	0.896959	0.983752	-0.70389	0.975459	56028.9	2.384834	309.3034	14121.95	2.948141	450.2057	1.09181
0.40277	488.6222	2.75243	0.89723	0.982979	-0.68463	0.971183	56926.79	2.306746	305.8082	14353.85	3.625603	475.4772	1.151343
0.41314	457.9086	2.45746	0.91593	0.984332	-0.72632	0.969142	57994.13	2.136332	303.2818	14613.01	2.837686	449.8562	0.935696
0.39308	456.5841	2.86565	0.89376	0.983803	-0.69998	0.976889	55922.31	2.433511	306.9553	14094.72	2.965049	447.7926	1.118605

0.37250 5	460.809 4	3.28267	0.865368	0.982737	-0.65926	0.979987	52927.63	2.713347	318.2102	13347.11	3.215505	450.47	1.337373
0.40277 7	488.622 2	2.75524 3	0.89723	0.982979	-0.68463	0.971183	56926.79	2.306746	305.8082	14353.85	3.625603	475.4772	1.151343
0.41220 4	464.141 1	2.53938 7	0.910581	0.984129	-0.70836	0.968653	58025.99	2.169121	302.0284	14622.53	3.205055	453.8687	1.016924
0.40577 1	449.170 9	2.65060 2	0.903197	0.984423	-0.70149	0.971058	57221.48	2.250298	302.6528	14417.66	3.073091	439.727	1.062636
0.41820 6	429.499 2	2.35880 3	0.92113	0.985426	-0.73677	0.967558	58512.14	2.060884	298.7474	14735.41	2.666309	422.39	0.887862
0.41197 4	433.434 7	2.51144 1	0.913711	0.985124	-0.72489	0.97081	57838.26	2.173814	300.8683	14567.92	2.755386	425.8425	0.951332
0.40966 5	435.136 4	2.55184 4	0.909715	0.98504	-0.71263	0.969898	57738.12	2.185116	300.4738	14543.31	2.878068	426.8531	0.997106
0.41517 8	424.815 6	2.42267 1	0.918121	0.985533	-0.73153	0.96894	58304.09	2.107963	299.6186	14682.23	2.658445	417.7483	0.911998
0.40804 7	431.014 1	2.59806 8	0.907225	0.985126	-0.71053	0.971038	57524.44	2.218981	302.7347	14488.86	2.87828	422.7296	1.018259
0.41832 5	429.238 8	2.35107	0.92141	0.985464	-0.73622	0.967152	58630.08	2.052434	297.7686	14764.83	2.649559	422.2186	0.882542
0.39989	448.412 8	2.77369 4	0.89532	0.984296	-0.68603	0.971994	56660.74	2.326259	304.6322	14277.29	3.208795	438.1165	1.136901
0.39583 6	472.397 1	2.86652 7	0.888746	0.983315	-0.67153	0.972043	56154.31	2.368448	305.8361	14156.68	3.536393	459.891	1.211653
0.39856 3	443.968 1	2.80033	0.895125	0.984442	-0.68693	0.972934	56627.93	2.352958	304.1372	14267.97	3.108565	434.3049	1.129873
0.41977 7	427.628	2.35810 4	0.921654	0.985516	-0.73615	0.967411	58620.55	2.056514	298.7917	14762.04	2.693389	420.3737	0.887137
0.42453 8	434.778 7	2.25592 8	0.927523	0.985383	-0.74623	0.9653	59054.81	1.984177	296.9634	14872.4	2.670393	427.6477	0.833817

0.41021	443.0046	2.532626	0.909838	0.984749	-0.7102	0.969016	57653.97	2.166808	300.6826	14524.24	2.932864	434.4029	1.000344
0.397846	472.1906	2.834216	0.891318	0.983318	-0.67582	0.9719	56138.3	2.3533	306.0684	14152.62	3.483997	460.0523	1.187131
0.400556	468.8776	2.778497	0.894437	0.9836	-0.67943	0.970916	56712.13	2.313557	305.8996	14295.25	3.554879	456.2405	1.171003
0.399083	484.6236	2.832042	0.891829	0.982977	-0.67405	0.971509	56451.77	2.348554	306.4492	14234.1	3.75461	470.5265	1.203873
0.424147	440.2207	2.262299	0.92538	0.98521	-0.73845	0.963971	59088.3	1.973617	296.9546	14882.13	2.818166	432.2786	0.865918
0.391707	490.0515	3.005197	0.88262	0.982536	-0.66154	0.974028	55630.04	2.473497	312.015	14030.02	3.787127	475.7092	1.278376
0.395822	483.054	2.904853	0.890306	0.983024	-0.6751	0.973754	56426.55	2.418807	308.5644	14227.4	3.62551	469.9097	1.210277
0.422541	448.2223	2.304308	0.923061	0.984926	-0.73222	0.964456	59020.14	2.001036	297.3306	14867.09	2.968749	439.4089	0.898056
0.404692	467.7411	2.725651	0.9002	0.983781	-0.69013	0.971299	57211.17	2.28904	305.6389	14419.73	3.503753	455.4384	1.126557
0.419487	449.4979	2.37922	0.919626	0.98481	-0.72605	0.966225	58735.11	2.05977	298.3544	14796.15	2.984796	440.5889	0.928726
0.421081	441.8009	2.36071	0.921651	0.985103	-0.73065	0.966423	58873.73	2.048937	298.5008	14828.8	2.968139	432.9911	0.914369
0.419424	463.7638	2.390291	0.919427	0.984349	-0.7275	0.966944	58801.05	2.073638	300.4343	14816.2	3.048318	454.4716	0.932419
0.397318	464.3534	2.858612	0.890636	0.983645	-0.67411	0.97229	56319.52	2.374393	307.6862	14195.97	3.54492	451.7869	1.203054
0.391825	500.5916	3.008942	0.882779	0.982209	-0.66321	0.974419	55773.53	2.478877	310.7112	14068.53	3.880541	485.533	1.282651
0.409282	468.9315	2.585874	0.90663	0.983841	-0.70168	0.968964	57572.45	2.19394	302.4116	14510.35	3.254043	458.3427	1.050665

0.39 760 4	482. 369 3	2.85 183 1	0.890 795	0.983 061	- 0.673 21	0.971 93	564 72.1 9	2.3685 04	305. 89	142 38.6 4	3.68 433 8	468. 794 9	1.207 8